$CD4^+$ T cells. The results obtained in the present study show for the first time the ability of HIV-1-specific $CD4^+$ CTLs to suppress HIV-1 replication in natural host cells, i.e., macrophages and $CD4^+$ T cells.

MATERIALS AND METHODS

Patients. Informed consent was obtained from all subjects, in accordance with the Declaration of Helsinki. Plasma and PBMCs were separated from heparinized whole blood. The patients were sampled at the AIDS Clinical Center, International Medical Center of Japan, and the HLA types of the patients were determined by standard sequence-based genotyping. Patients with active opportunistic infections or psychological disorders and those treated with immunomodulatory agents were excluded.

Synthetic peptides. Peptides (17-mer) derived from the consensus sequence of the Nef protein of HIV-1 clade B were synthesized. These 17-mer peptides overlapped each other by 11 residues. For the feasibility of screening for T-cell epitopes, eight peptides were pooled in a cocktail. Peptides were prepared by using an automated multiple peptide synthesizer. The purity of the synthesized peptides was examined by mass spectrometry, and the peptides with >90% purity were used in the present study.

Cell surface and intracellular cytokine staining. For detection of intracellular cytokines of $CD4^+$ T cells, PBMCs or Nef-specific $CD4^+$ T-cell clones (effector cells) bulk cultured with peptides were stimulated with autologous EBV-transformed B-lymphoblastoid cells (B-LCLs) prepulsed with Nef-derived peptides or peptide cocktails (10^{-6} M) at an effector-to-stimulator (E/S) ratio of 1:4. The pulsed stimulator cells were washed twice in RPMI 1640–10% fetal calf serum (FCS) before use. The mixed cells were incubated for 6 h at 37°C in 5% CO_2. Brefeldin A (Sigma-Aldrich) was added at a concentration of 10 μg/ml after the first 2 h of incubation to inhibit secretion of cytokines. In order to determine the MHC-II restriction of the $CD4^+$ T-cell epitopes, we also employed peptide-pulsed allogeneic B-LCLs with the HLA-DR allele partially matched or mismatched as stimulators in some assays. After a 6-hour incubation, the cells were stained with phycoerythrin (PE)-conjugated anti-human CD4 monoclonal antibody (MAb) (BD Biosciences, San Jose, CA). Then the cells were fixed, made permeable, stained with fluorescein isothiocyanate (FITC)-conjugated anti-human gamma interferon (IFN-γ) MAb (BD Biosciences, San Jose, CA), and analyzed by flow cytometry as previously described (16).

In order to determine the expression of cytotoxic effector molecules, we directly stained PBMCs or Nef-specific $CD4^+$ T-cell clones with allophycocyanin (APC)-conjugated anti-human CD4 or PE-conjugated anti-human CD4 MAb (BD Biosciences, San Jose, CA) without any stimulation of the cells. Then the cells were fixed, made permeable, stained with FITC-conjugated anti-human perforin, PE-conjugated anti-human granzyme A, or Alexa 647-conjugated anti-human granzyme B MAb (BD Biosciences, San Jose, CA), and analyzed by flow cytometry as previously described (44).

To detect the degranulation of Nef-specific $CD4^+$ T cells following antigen stimulation directly ex vivo, we incubated PBMCs with PE-conjugated anti-human CD107a MAb or PE-conjugated isotype control MAb in RPMI 1640–10% FCS containing the corresponding peptide (10^{-6} M), as previously described by Casazza et al. (10). Negative controls containing the PBMCs from the same individual but without peptides were also prepared. Cells were incubated for 6 h at 37°C in 5% CO_2. Brefeldin A was added at a concentration of 10 μg/ml after the first 2 h of incubation. Then, the cells were stained with APC-conjugated anti-human CD4 MAb and FITC-conjugated anti-human IFN-γ MAb and analyzed as described above.

Generation of Nef-specific $CD4^+$ T-cell clones. Peptide-specific $CD4^+$ T-cell clones were generated from an established peptide-specific bulk $CD4^+$ T-cell culture by limiting dilution in U-bottom 96-well microtiter plates (Nunc, Roskilde, Denmark) together with 200 μl of cloning mixture (RPMI 1640 medium supplemented with 10% human serum from healthy donors and 200 U/ml recombinant human IL-2, 5×10^4 irradiated allogeneic PBMCs from a healthy donor as feeders, and 1×10^5 irradiated autologous EBV-transformed B-LCLs prepulsed with a 10^{-6} M concentration of the corresponding peptide). Wells positive for growth after 2 to 3 weeks were transferred to 48-well plates together with 1 ml of the cloning mixture. The clones were examined for specific IFN-γ-producing ability by intracellular cytokine staining. All $CD4^+$ T-cell clones were cultured in RPMI 1640–10% human serum from healthy donors supplemented with 200 U of recombinant human IL-2/ml and were stimulated weekly with irradiated autologous B-LCLs prepulsed with the appropriate epitope peptide.

Blocking of $CD4^+$ T-cell responses. To determine the MHC-II restriction of Nef-specific $CD4^+$ T-cell responses, we blocked the T-cell receptor–MHC-II interaction by using human MHC-II molecule-specific MAbs L243 (anti-HLA-DR), B7/21 (anti-HLA-DP), and Hu-11 and Hu-18 (anti-HLA-DQ4+5+6 and anti-HLA-DQ7+8+9, respectively), which were kindly donated by Y. Nishimura. Autologous B-LCLs prepulsed with the Nef epitope were incubated with the appropriate antibody (10 μg/ml) for 1 h on ice. Subsequently, the cells were washed in RPMI 1640–10% FCS and then incubated with Nef-specific $CD4^+$ T-cell clones (effector cells) at an E/S ratio of 1:2 for 6 h. Brefeldin A was added to the cultures (10 μg/ml) 4 h prior to termination of the cultures. To evaluate the ability of the effector cells to produce IFN-γ under blocking conditions, we stained the cells after stimulation with PE-conjugated anti-human CD4 MAb. Then the cells were fixed, made permeable, and stained with FITC-conjugated anti-human IFN-γ, as described above.

Intracellular cytokine production (ICC) assays for stimulator cells infected with recombinant vaccinia virus. Autologous B-LCLs were infected with 10 PFU per cell of recombinant vaccinia virus expressing HIV-1 Nef (rVac-Nef) or wild-type vaccinia virus (Vac-WT) and cultured for 16 h at 37°C in 5% CO_2. The infected cells were washed twice with RPMI 1640–10% FCS and then incubated with Nef-specific $CD4^+$ T-cell clones (effector cells) at an E/S ratio of 1:4 for 6 h. Brefeldin A was present in the cultures (10 μg/ml) for the last 4 h. To evaluate the ability of the effector cells to produce IFN-γ, we stained the cells with PE-conjugated anti-human CD4 MAb after stimulation. Then the cells were fixed, made permeable, and stained with FITC-conjugated anti-human IFN-γ, as described above.

ICC assays for stimulator cells pulsed with heat-inactivated HIV-1 particles. The virus particles of HIV-1 NL-432 and its Nef-defective mutant were generated by the HIV-1 clones and were heat inactivated at 56°C for 30 min. Autologous B-LCLs were incubated with the inactivated virus particles at 0.5 μg/ml (p24 antigen concentration) for 16 h at 37°C in 5% CO_2. The pulsed cells were washed twice with RPMI 1640–10% FCS and then incubated with Nef-specific $CD4^+$ T-cell clones (effector cells) at an E/S ratio of 1:4 for 6 h. Brefeldin A was present in the cultures (10 μg/ml) for the last 4 h. To evaluate the ability of effector cells to produce IFN-γ after stimulation, we sequentially stained the cells with PE-conjugated anti-human CD4 MAb, fixed them, made them permeable, and then stained them with FITC-conjugated anti-human IFN-γ MAb, as described above.

ICC assay for stimulator cells transfected with Nef-GFP fusion mRNA. For stimulator cells endogenously expressing Nef-green fluorescent protein (GFP) fusion proteins, m7GpppG-capped and poly(A)-tailed Nef-GFP fusion mRNA or GFP mRNA was delivered to autologous B-LCLs by electroporation, as previously described (46). Briefly, B-LCLs were suspended in a serum-free medium (Opti-MEM; Invitrogen Life Technologies) at the cell density of 2×10^6 cells/ml, mixed with 10 μg of mRNA, and electroporated by using a Gene Pulser device (Bio-Rad). The cells were immediately transferred to RPMI 1640–10% FCS, incubated at 37°C for 1.5 to 3 h, and then mixed with Nef-specific $CD4^+$ T-cell clones (effector cells) at an E/S ratio of 1:4. B-LCLs transfected with GFP mRNA were prepared as negative controls. Flow cytometry revealed that more than 60% of the viable B-LCLs expressed GFP. The cell mixtures were incubated for 6 h, and brefeldin A (10 μg/ml) was present for the last 4 h of the incubation. To evaluate the ability of the effector cells to produce IFN-γ after stimulation, we performed surface and intracellular cytokine staining to the cells, as described above.

Isolation and culture of macrophages and $CD4^+$ T cells. Monocytes and $CD4^+$ T cells were isolated from PBMCs of an HLA-DRB1*0803-positive or HLA-DRB1*0403-positive healthy donor by using anti-human CD14 MAb-coated and anti-human CD4 MAb-coated magnetic beads (magnetically activated cell sorting beads; Miltenyi Biotec, Bergisch Gladbach, Germany), respectively. The isolated monocytes were cultured in complete medium containing macrophage colony-stimulating factor (50 ng/ml) for 1 week before use. The isolated $CD4^+$ T cells were cultured for 1 week in complete medium containing IL-2 (200 U/ml) and IL-4 (2.5 ng/ml) and stimulated with OKT3 anti-CD3 MAb (10 μg/ml) every 3 days during the culture period. These cultured macrophages and $CD4^+$ T cells were infected with HIV-1 as previously described (17, 45).

HIV-1 clones. Infectious proviral clones of an X4 HIV-1, pNL-432, and its Nef-defective mutant, pNL-Xh, which has a frameshift at a XhoI site (44th amino acid of the Nef protein), were kindly donated by Y. Koyanagi (Kyoto University, Kyoto, Japan). The infectious proviral clone of $pJRFL_{NL\text{-}432Nef}$ was previously constructed by exchanging the Nef region of R5 strain JRFL with that of NL-432 (17).

CTL assay. The cytotoxicity of Nef-specific $CD4^+$ T-cell clones against B-LCLs or HIV-1-infected target cells was measured by a standard ^{51}Cr release assay as previously described (17). Briefly, target cells (2×10^5) were incubated for 60 min with 100 μCi of $Na_2{}^{51}CrO_4$ in saline and washed three times with RPMI 1640 medium containing 10% NCS. Labeled target cells (2×10^3/well)

were seeded in a 96-well round-bottom microtiter plate (Nunc). For the assays of B-LCLs, the desired amount of the corresponding peptide was coincubated with labeled target cells for 1 h. Then, effector cells were added at various E/T ratios, and the mixtures were incubated for 4 h at 37°C. The supernatants were collected and analyzed with a gamma counter. The spontaneous ^{51}Cr release was determined by measuring the cpm in the supernatant in the wells containing only target cells (cpm spn). Maximum release was determined by measuring the release of ^{51}Cr from the target cells in the presence of 2.5% Triton X-100 (cpm max). Specific lysis was calculated by using the formula (cpm exp − cpm spn)/(cpm max − cpm spn) × 100 (%), where cpm exp is the counts per minute in the supernatant in the wells containing both target and effector cells.

Suppression of HIV-1 replication by HIV-1-specific CTLs. The ability of HIV-1 Nef-specific $CD4^+$ CTLs to suppress HIV-1 replication was examined as previously described (45). Briefly, macrophages or $CD4^+$ T cells were incubated with a given HIV-1 clone for 6 h at 37°C in 5% CO_2. After two washes with RPMI 1640–10% FCS, the cells were cocultured with the $CD4^+$ CTL clones. From days 3 to 9 after infection, 10 μl of culture supernatant was collected, and the concentration of p24 antigen was measured by use of an enzyme immunoassay (HIV-1 p24 antigen enzyme-linked immunosorbent assay kit (ZeptMetrix, Buffalo, NY). The percentage of suppression of HIV-1 replication was calculated as follows: % suppression = (1 − concentration of p24 Ag in the supernatant of HIV-1-infected cells cultured with HIV-1-specific CTLs/concentration of p24 Ag in the supernatant of HIV-1-infected cells culture without the CTLs) × 100.

RESULTS

Identification and characterization of two HIV-1 Nef-specific $CD4^+$ T-cell epitopes. PBMC from two HIV-1-seropositive individuals, KI-010 and KI-197, were cultured for 14 days after stimulation with either of four peptide cocktails comprising eight 17-mer overlapping Nef peptides. Specific IFN-γ production by each PBMC culture was tested by using intracellular IFN-γ staining after restimulating the cells with autologous EBV-transformed B-LCLs prepulsed with the corresponding peptide cocktail. Cocktail 1 and cocktail 4 induced specific IFN-γ-producing $CD4^+$ T cells among the PBMCs from KI-010 and KI-197, respectively (Fig. 1A). In order to determine which peptide was responsible for the specific $CD4^+$ T-cell responses in the peptide cocktails, we subsequently stimulated the responding PBMC cultures with autologous B-LCLs pulsed with each peptide included in the corresponding peptide cocktails. Nef17-7 and Nef17-8 peptides induced specific $CD4^+$ T-cell responses by the PBMCs cultured from KI-010, whereas Nef17-31 and Nef17-32 peptides induced specific ones by those from KI-197 (Fig. 1B). Considering that the flanking residues also contribute a small part to the overall binding energy of MHC-II-binding peptides, the core binding region is usually not the optimal ligand for MHC-II molecules. Therefore, we used the full-length 17-mer peptides Nef37-53 (Nef17-7) and Nef187-203 (Nef17-32) to generate $CD4^+$ T-cell clones for further studies. The clones specific for Nef37-53 and Nef187-203 epitopes were generated from KI-010 and KI-197, respectively.

In order to determine the HLA class II restriction molecules of these two $CD4^+$ T-cell epitopes, we employed HLA-DR-, -DP-, and -DQ-specific MAbs to block the T-cell receptor-HLA class II interaction between Nef-specific $CD4^+$ T cells and the stimulator cells. HLA-DR-specific MAb L243 blocked the recognition by both Nef37-53- and Nef187-203-specific $CD4^+$ T-cell clones after stimulation with the peptide-pulsed autologous B-LCLs, whereas HLA-DQ-specific MAb Hu11 or Hu18 and HLA-DP-specific MAb B7/21 failed to block it (Fig. 1C). These results indicate that these two epitope-specific T-cell responses were restricted by HLA-DR. To determine the

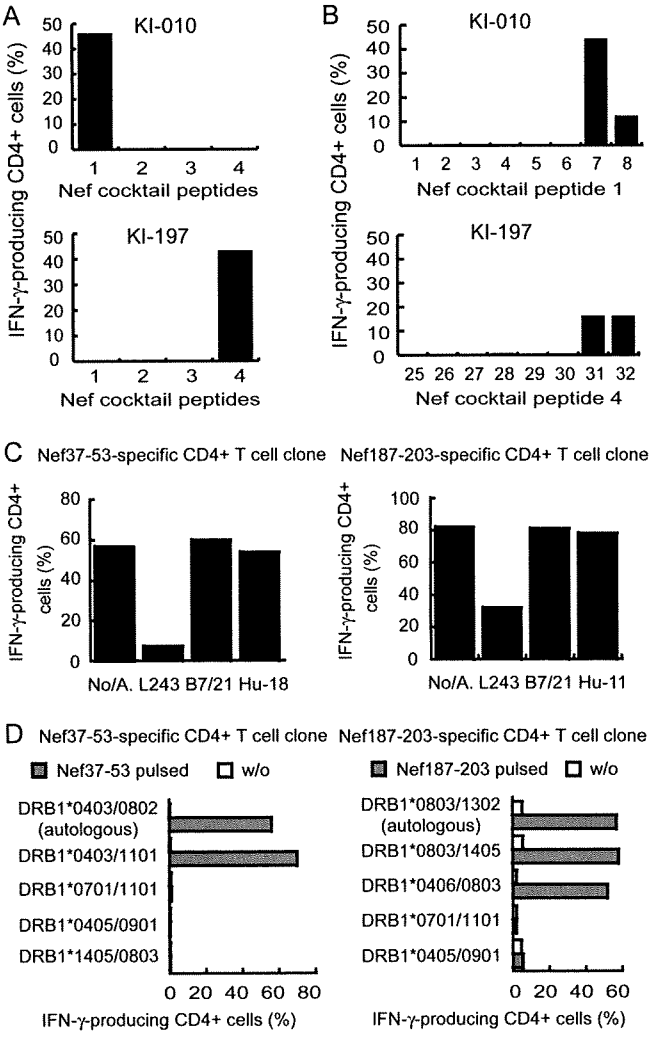

FIG. 1. Identification and characterization of two HIV-1 Nef-specific $CD4^+$ T-cell epitopes. (A) Induction of Nef-specific $CD4^+$ T cells from PBMCs of HIV-1-infected individuals. PBMCs from two HIV-1-seropositive donors (KI-010 and KI-197) were stimulated with cocktails comprising eight 17-mer overlapping Nef peptides and then were cultured for 2 weeks. IFN-γ-producing $CD4^+$ T cells (%) among these bulk-cultured PBMCs were detected by intracellular staining for IFN-γ after restimulation with autologous B-LCLs pulsed with the same cocktails. (B) IFN-γ-producing $CD4^+$ T cells induced by Nef single peptides. The PBMC bulk cultures that responded to the peptide cocktails were subsequently stimulated with B-LCLs pulsed with individual peptides included in those cocktails. IFN-γ-producing $CD4^+$ T cells (%) induced by single peptides were detected by intracellular staining for IFN-γ. (C) IFN-γ responses of Nef37-53-specific and Nef187-203-specific $CD4^+$ T-cell clones to the stimulation with peptide-pulsed B-LCLs were blocked by HLA-DR-specific antibody. Autologous B-LCLs prepulsed with epitope peptides were incubated with MHC-II-specific antibodies (No/A., no antibody; L243, anti-HLA-DR; B7/21, anti-HLA-DP; Hu11 and Hu18, anti-HLA-DQ) for 1 h. Then the two Nef epitope-specific $CD4^+$ T-cell clones were stimulated with the MHC-II-specific antibody-treated B-LCLs at an E/S ratio of 1:2. The percentage of IFN-γ-producing cells in the Nef-specific $CD4^+$ T-cell clones after stimulation was determined by intracellular staining for IFN-γ. (D) IFN-γ responses of Nef37-53-specific and Nef187-203-specific $CD4^+$ T-cell clones after stimulation with peptide-pulsed autologous B-LCL or peptide-pulsed allogeneic B-LCLs with partially matched and mismatched HLA-DR. The percentage of IFN-γ-producing cells among the Nef-specific $CD4^+$ T-cell clones after stimulation was determined by intracellular staining for IFN-γ.

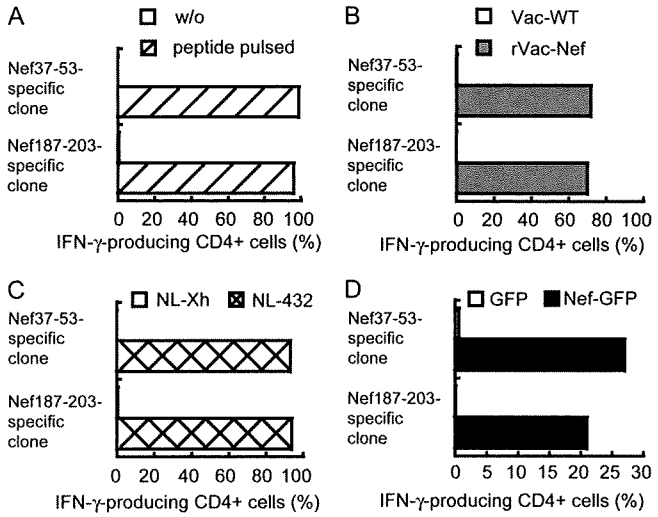

FIG. 2. Naturally occurring presentation of CD4+ T-cell epitopes. Nef37-53-specific and Nef187-203-specific CD4+ T-cell clones were stimulated with peptide-pulsed, recombinant vaccinia virus-infected, HIV-1 particle protein-pulsed, or Nef-GFP fusion mRNA-transfected autologous B-LCLs. The percentage of IFN-γ-producing cells among the Nef-specific CD4+ T-cell clones after stimulation was determined by intracellular staining for IFN-γ. (A) Nef-specific CD4+ T-cell clones were tested for their IFN-γ production after stimulation with B-LCLs prepulsed with appropriate epitope peptides (peptide pulsed) or those without peptides (w/o). (B) Nef-specific CD4+ T-cell clones were tested for IFN-γ production after stimulation with B-LCLs infected with rVac-Nef or Vac-WT. (C) Nef-specific CD4+ T-cell clones were tested for their IFN-γ production after stimulation with B-LCLs prepulsed with heat-inactivated HIV-1 particles of X4 strain NL-432 (NL-432) or those of its Nef-defective mutant, NL-Xh (NL-Xh). (D) Nef-specific CD4+ T-cell clones were tested for their IFN-γ production after stimulation with Nef-GFP fusion mRNA-transfected B-LCLs (Nef-GFP) or GFP mRNA-transfected B-LCLs (GFP). Approximately 60% of the stimulator cells were Nef+ or GFP+ cells.

exact restriction alleles, we stimulated Nef37-53-specific and Nef187-203-specific CD4+ T-cell clones with peptide-prepulsed B-LCLs from allodonors with partially matched or mismatched HLA-DR. The Nef37-53-specific CD4+ T-cell clone produced IFN-γ after stimulation with the corresponding peptide-pulsed B-LCLs from the donors sharing DRB1*0403, while the Nef187-203-specific clone produced IFN-γ after stimulation with the corresponding peptide-pulsed B-LCLs from the donors sharing DRB1*0803 (Fig. 1D). These results strongly suggest that the restriction alleles of CD4+ T-cell epitopes Nef37-53 and Nef187-203 were HLA-DRB1*0403 and HLA-DRB1*0803, respectively.

Naturally occurring presentation of CD4+ T-cell epitopes in rVac-Nef-infected or HIV-1 Nef protein-pulsed cells. To clarify the naturally occurring presentation of these two Nef epitopes, we investigated the ability Nef37-53-specific and Nef187-203-specific CD4+ T-cell clones to produce IFN-γ after stimulation of them with autologous B-LCLs infected with rVac-Nef or those pulsed with heat-inactivated virus particles. The Nef37-53-specific and Nef187-203-specific clones used in this assay showed similar abilities to produce IFN-γ (>95%) after the stimulation with peptide-pulsed autologous B-LCLs (Fig. 2A). The B-LCLs infected with rVac-Nef induced about 70% of the two Nef-specific CD4+ T-cell clones to produce IFN-γ, whereas those cells infected with Vac-WT did not induce any IFN-γ production (Fig. 2B). In addition, the B-LCLs pulsed with NL-432 virus particles induced more than 90% of the CD4+ T cells from the Nef-specific clones to produce IFN-γ, whereas those cells pulsed with NL-Xh (Nef-depleted) virus particles failed to induce IFN-γ production (Fig. 2C). This result suggests that the Nef-specific CD4+ T cells also recognized the epitope antigen presented through endogenous MHC-II processing pathways. However, it still remains possible that Nef proteins from cells expressing Nef killed by vaccinia virus or HIV infection were presented by the exogenous HLA class II pathway. To exclude this possibility, we used stimulator cells transfected with Nef-GFP mRNA. Nef-GFP mRNA-transfected autologous B-LCLs induced IFN-γ production from both Nef37-53-specific and Nef187-203-specific CD4+ T-cell clones, whereas GFP mRNA-transfected cells did not (Fig. 2D). In this assay, B-LCLs were used as stimulator cells within 3 h after the transfection. The frequency of dead cells among the Nef+ cells was approximately 0.6%. These results support the idea that endogenous HIV-1 Nef can be processed to MHC-II molecules in a manner similar to that of the previously observed endogenous presentation of HCMV CD4+ CTL epitopes (20). Thus, our results indicate that the Nef-specific CD4+ T cells recognized the epitope antigen presented through both exogenous and endogenous MHC-II processing pathways.

Cytotoxic activity and cytotoxic effector molecule expression of HIV-1 Nef-specific CD4+ T cells. Although antigen-specific CD4+ T cells are classically thought to function as helper T cells in antiviral immunity, HIV-1 Gag-specific cytotoxic CD4+ T cells were previously reported to exist (30–32, 50). In our study, Nef37-53-specific and Nef187-203-specific CD4+ T-cell clones were tested for their ability to lyse autologous B-LCLs incubated with the epitope peptide (1,000 nM) at an E/T ratio of 5:1 (Fig. 3A). The Nef187-203-specific CD4+ T-cell clone showed a strong lytic activity against autologous B-LCLs incubated with the peptide, whereas the Nef37-53-specific CD4+ T-cell clone did not lyse autologous B-LCLs pulsed with the peptide. Furthermore, we stained for three cytotoxic effector molecules in these Nef-specific CD4+ T-cell clones and found that the expression levels of perforin and granzyme B were much higher in the Nef187-203-specific clone than in the Nef37-53-specific one, whereas the two clones showed similar levels of granzyme A expression (Fig. 3B). Considering that Th clones have been shown to develop cytotoxic activity after long-term culture in vitro (15), we sought to detect the cytotoxic activity of these two Nef epitope-specific CD4+ T cells ex vivo. We employed flow cytometric analysis to measure the cell surface mobilization of CD107a (6, 14), because only a very small number of these epitope-specific CD4+ T cells are suspected to exist among the PBMCs of these patients; thus, these cells would fail to kill the target cells in a chromium release assay. Epitope-specific CD4+ T cells among the PBMCs from two HIV-1-seropositive donors, KI-010 and KI-197, could be detected at very low frequency by revealing their specific IFN-γ responses following peptide stimulation for 6 h (Fig. 3C). We then gated the IFN-γ-producing CD4+ T cells and compared the levels of cell surface expression of CD107 for these two types of CD4+ T cells. The results showed that about 50% of Nef187-203-specific CD4+ T cells expressed CD107a on their

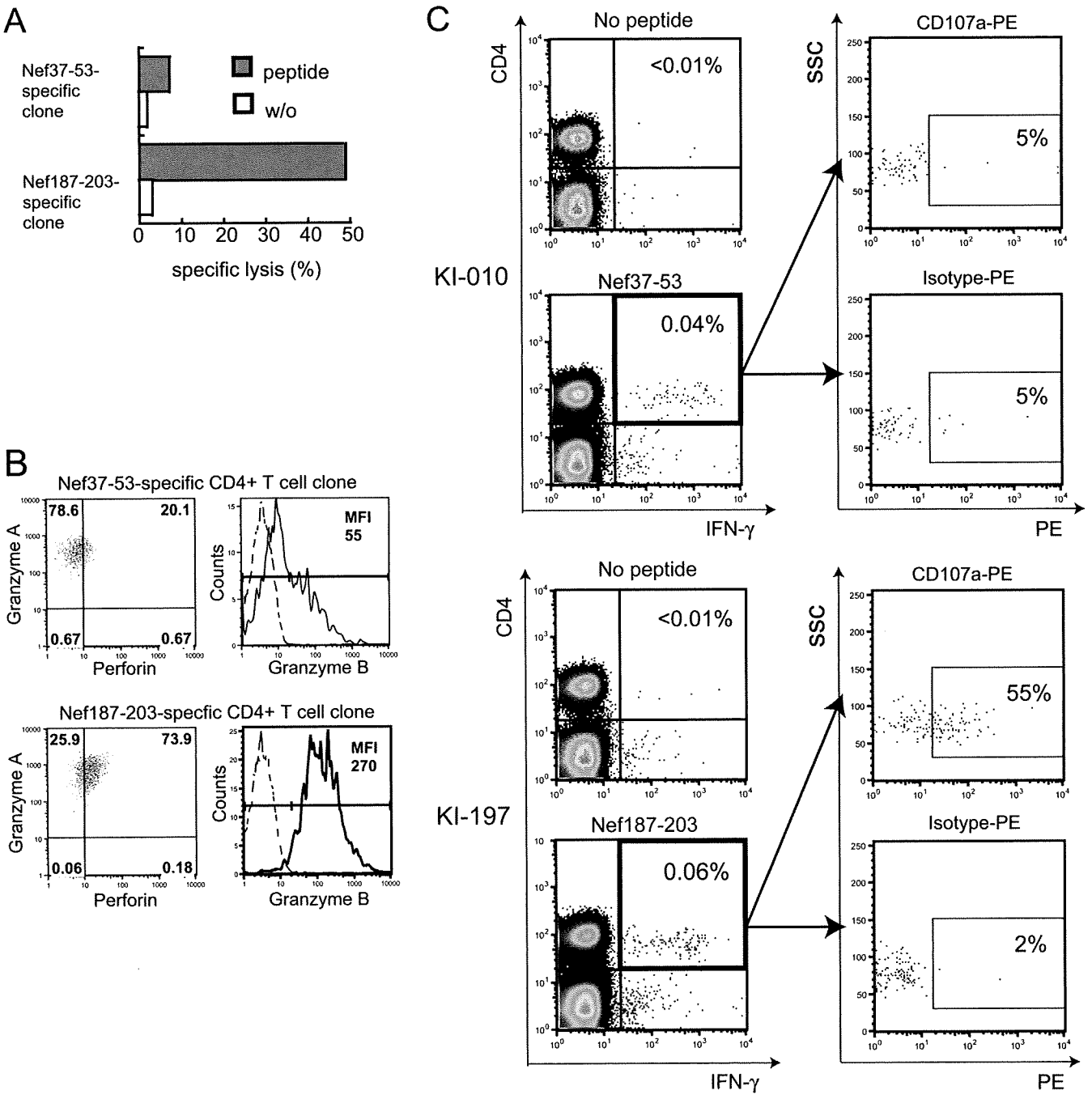

FIG. 3. Cytotoxic activity and cytotoxic effector molecule expression of HIV-1 Nef-specific $CD4^+$ T cells. (A) Cytotoxic activities of a KI-010-derived Nef37-53-specific $CD4^+$ T-cell clone and a KI-197-derived Nef187-203-specific $CD4^+$ T-cell clone against autologous B-LCLs incubated with the epitope peptides (1,000 nM) were measured by a standard ^{51}Cr release assay at an effector-to-target ratio of 5:1. Peptide, with peptide; w/o, without peptide. (B) Surface staining for CD4 and intracellular staining for perforin, granzyme A, and granzyme B were carried out on the Nef37-53-specific and Nef187-203-specific $CD4^+$ T-cell clones. The clones were stained without any stimulation. The stained clones were analyzed by flow cytometry, and the $CD4^+$ cells were gated. The expression levels of perforin and granzyme A are shown in dot plots. Values in dot plots show the frequencies (%) of the subsets among the $CD4^+$ T-cell clones. The expression levels of granzyme B are shown in histograms. Solid lines show the clones stained with anti-human granzyme B MAb; dashed lines show the same clones stained with isotype control antibody. Values in histograms show mean fluorescence intensities (MFI) of the solid lines. (C) Ex vivo analysis of CD107a surface expression on Nef37-53-specific and Nef187-203-specific $CD4^+$ T cells. PBMCs from two HIV-1-seropositive donors, KI-010 and KI-197, were incubated with or without their corresponding epitope peptide for 6 h. Then these PBMCs were stained with anti-CD4, anti-IFN-γ, and anti-CD107a or with mouse immunoglobulin G (IgG) MAb as an isotype control. Values in the IFN-γ/CD4 dot plots indicate the frequencies of IFN-γ-producing $CD4^+$ cells. The $CD4^+$ IFN-γ^+ cells in each PBMC population were gated, and then they were analyzed for the surface expression of CD107a. Values in the PE/side scatter (SSC) dot plots indicate the frequencies of the high-fluorescence subsets in the gated $CD4^+$ IFN-γ^+ population of the PBMCs stained with PE-conjugated anti-CD107a (CD107a-PE) and of the same PBMCs stained with PE-conjugated mouse IgG isotype MAb (Isotype-PE).

cell surfaces, whereas Nef37-53-specific CD4+ T cells did not, thus indicating that Nef187-203-specific CD4+ CTLs, but not Nef37-53-specific CD4+ T cells, have the ability to function as cytotoxic T cells.

Lysis of HIV-1-infected macrophages and CD4+ T cells by Nef187-203-specific cytotoxic CD4+ T cells. To investigate if the Nef-specific CD4+ T cells were able to kill HIV-1-infected target cells, we measured their cytotoxic activity against HIV-1-infected macrophages and CD4+ T cells. To exclude the possibility that different Nef sequences between two HIV-1 strains, NL-432 and JRFL, would affect the recognition of Nef-specific CD4+ CTLs, we used $JRFL_{NL\text{-}432Nef}$, a chimera R5 virus, with the Nef protein derived from the NL-432 strain in this study. Macrophages and CD4+ T cells from an HLA-DRB1*0803-positive healthy donor were infected with HIV-1 R5 strain $JRFL_{NL\text{-}432Nef}$ and X4 strain NL-432, respectively. Intracellular p24 staining of these cells showed that more than 80% of the cultured macrophages and CD4+ T cells were p24 antigen positive at day 3 postinfection, indicating the establishment of an HIV-1 infection in the cultured cells (Fig. 4A). Three Nef187-203-specific CD4+ CTL clones were used in our assays. They exhibited strong specific lysis of autologous B-LCLs incubated with 1,000 nM peptide; this lysis was dramatically decreased when the B-LCLs were incubated with 100 nM peptide (Fig. 4B), thus showing a lower sensitivity of peptide-pulsed target cells to Nef-specific CD4+ CTL clones than that of Nef-specific CD8+ CTL clones reported in our previous studies (18, 46). These Nef-specific CD4+ CTL clones killed both HIV-1-infected macrophages and CD4+ T cells, even at a decreased E/T ratio of 2:1 (Fig. 4C). The specific lysis of infected macrophages was higher than that of the infected CD4+ T cells. This difference may result from the intracellular p24 antigen expression levels of these two targets used in this assay (Fig. 4A).

Ability of HIV-1 Nef-specific cytotoxic CD4+ T cells to suppress HIV-1 replication in macrophages and CD4+ T cells. A previous study showed that Gag-specific CD4+ CTLs can suppress HIV-1 replication in human T-cell leukemia virus type 1-immortalized CD4+ T-cell line MT-2 (31). To clarify if CD4+ CTLs could also efficiently suppress HIV-1 replication in its natural host cells in vivo, we measured the ability of Nef-specific CD4+ CTLs to suppress the replication of HIV-1 in HIV-1-infected macrophages and CD4+ T cells in vitro. Macrophages and CD4+ T cells from an HLA-DRB1*0803-positive healthy donor were isolated, cultured, and then infected with HIV-1 $JRFL_{NL\text{-}432Nef}$ and NL-432 in vitro, respectively. To investigate the suppression ability of CD4+ CTLs by using an enzyme immunoassay, we measured p24 antigens in the supernatant of cultured HIV-1-infected target cells with or without a Nef187-203-specific CD4+ CTL clone at an E/T ratio of 0.1:1 (Fig. 5A). Two Nef187-203-specific clones revealed a strong ability to suppress HIV-1 replication in both HIV-1-infected macrophages and CD4+ T cells. The suppression ability of these T cell clones was E/T ratio dependent for both HIV-1-infected macrophages and CD4+ T cells (Fig. 5B), whereas the addition of an HLA class II-mismatched Nef37-53-specific CD4+ T-cell clone to HIV-1-infected macrophages or CD4+ T cells did not cause any suppression of p24 production (data not shown). Complete suppression of p24 production in both HIV-1-infected macrophages and CD4+ T cells

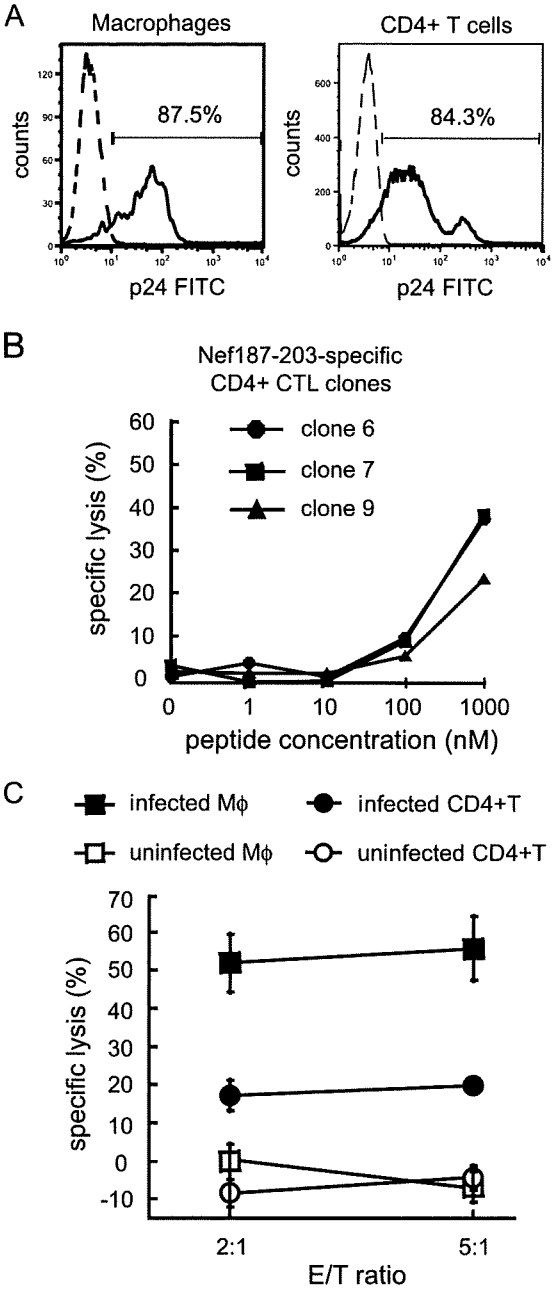

FIG. 4. Lysis of HIV-1-infected macrophages and CD4+ T cells by Nef187-203-specific cytotoxic CD4+ T cells. (A) Intracellular p24 antigen expression of macrophages and CD4+ T cells from an HLA-DRB1*0803-positive donor at day 3 postinfection. The dashed histogram represents uninfected cells, and the solid histogram represents HIV-1-infected cells. The values in each plot show the frequencies of p24 antigen-positive cells. The uninfected and HIV-1-infected macrophages and CD4+ T cells were then labeled with $Na_2{}^{51}CrO_4$ and incubated with Nef187-203-specific clones for CTL assays. (B) Cytotoxic activity of three Nef187-203-specific clones against autologous B-LCLs incubated with the peptide at the indicated concentrations. The cells were tested at an effector-to-target (E/T) ratio of 5:1. (C) Ability of Nef187-203-specific clones to lyse HIV-1-infected or uninfected macrophages (Mϕ) and CD4+ T cells. The cells were tested at the indicated E/T ratios by using the standard ^{51}Cr assay. Values represent averages ± standard deviations (error bars) of results from the assays of the three Nef187-203-specific clones.

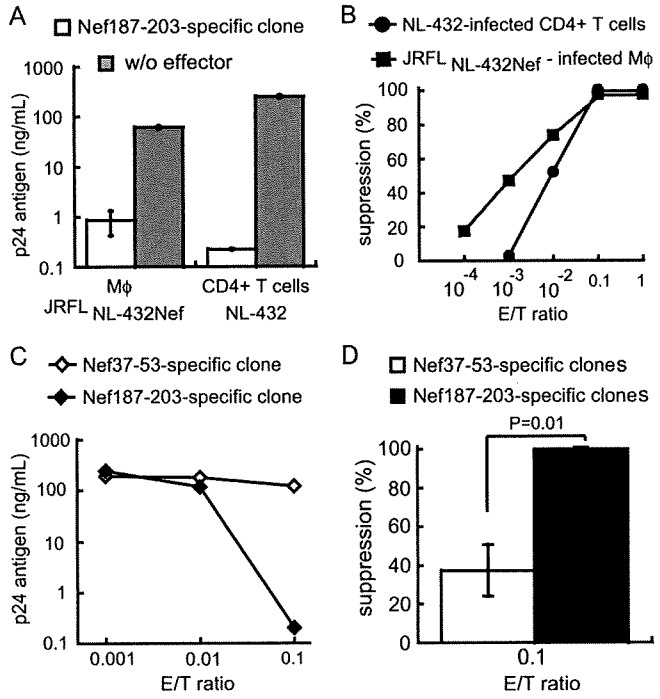

FIG. 5. Ability of HIV-1 cytotoxic CD4$^+$ T cells to suppress HIV-1 replication in vitro. (A) Ability of Nef187-203-specific CD4$^+$ CTL clones to suppress $JRFL_{NL\text{-}432Nef}$ virus and NL-432 virus replication in macrophages and CD4$^+$ T cells, respectively. Macrophages and CD4$^+$ T cells from an HLA-DR-compatible healthy donor were infected with HIV-1 and subsequently cocultured or not with Nef-187-203-specific CD4$^+$ CTL clones at an effector-to-target (E/T) ratio of 0.1:1. The concentration of p24 antigen in the supernatant on day 6 postinfection was measured by using an enzyme immunoassay. Values are presented as the averages ± standard deviations of results from the assays of two Nef187-203-specific clones. (B) The ability of Nef187-203-specific CD4$^+$ CTL clone to suppress HIV-1 infection in target cells was E/T ratio dependent. $JRFL_{NL\text{-}432Nef}$-infected macrophages or NL-432-infected CD4$^+$ T cells were subsequently cocultured with a Nef187-203-specific clone at the indicated E/T ratios. The concentration of p24 antigen in the supernatant on day 6 postinfection was measured as described above. (C) Ability of a Nef37-53-specific CD4$^+$ T-cell clone with no CTL activity to suppress HIV-1 replication in HIV-1-infected CD4$^+$ T cells. CD4$^+$ T cells from two healthy donors expressing the corresponding HLA-DR alleles were infected with HIV-1 and were subsequently cocultured with a Nef37-53-specific or Nef187-203-specific clone at the indicated E/T ratios. The concentration of p24 antigen in the supernatant on day 6 postinfection was measured as described above. (D) The ability of Nef37-53-specific CD4$^+$ T-cell clones to suppress HIV-1 replication in HIV-1 infected CD4$^+$ T cells was less than that of Nef187-203-specific CD4$^+$ CTL clones. Values are presented as averages ± standard deviations (error bars) of results from the assays of three Nef37-53-specific or Nef187-203-specific clones. Statistical differences were determined with Student's t test, and the double-sided P value is shown.

was detected at a low E/T ratio of 0.1:1, indicating that these Nef-specific CD4$^+$ CTLs had a very strong ability to suppress HIV-1 replication. To investigate if this strong suppressor ability could be attributed to the cytolytic activity of CD4$^+$ T cells, we compared the suppressor ability of Nef37-53-specific CD4$^+$ T cells, which did not show significant CTL activity, with that of the Nef187-203-specific CTL clones. A Nef37-53-specific clone with no CTL activity revealed weak suppression activity at an E/T ratio of 0.1:1 against the HIV-1-infected CD4$^+$ T cells from an HLA-compatible healthy donor (Fig. 5C), with this ability being significantly lower than that of the Nef187-203-specific CD4$^+$ CTL clone (Fig. 5D). This result indicates that the Nef-specific cytotoxic CD4$^+$ T cells have strong ability to suppress HIV-1 replication and that noncytotoxic Nef-specific CD4$^+$ T cells may have weak ability to suppress HIV replication via cytokines or by some other mechanism(s).

Detection of Nef187-203-specific CD4$^+$ T cells in chronically HIV-1-infected individuals. To investigate if CD4$^+$ T cells specific for Nef187-203 could be frequently found in HLA-DRB1*0803-positive HIV-1-infected individuals, we expanded our investigation to include nine more chronically HIV-1-infected patients carrying the HLA-DRB1*0803 allele. PBMCs from these patients and KI-197 were stimulated with Nef187-203 peptide and cultured for 2 weeks to expand the population of epitope-specific CD4$^+$ T cells. IFN-γ-producing cells were determined by intracellular staining after restimulation of the bulk cultures with HLA-DRB1*0803-positive B-LCLs prepulsed with the peptide. We observed Nef187-203-specific CD4$^+$ T cells in the bulk cultures from three of these nine donors, i.e., KI-105, KI-121, and KI-154. Taken together, our data indicate that Nef187-203-specific CD4$^+$ T cells were detected among cultured PBMCs from 4 of 10 HLA-DRB1*0803-positive HIV-1-infected individuals (Table 1).

Among the PBMCs from donors KI-154 and KI-197, who showed strong CD4 responses tested by the assay using in vitro-cultured PBMCs, we also detected Nef187-203-specific CD4$^+$ T cells directly ex vivo (Table 1). Furthermore, more than 50% of the Nef187-203-specific CD4$^+$ T cells from both KI-154 and KI-197 mobilized CD107a after stimulation with Nef187-203 peptide (Table 1), demonstrating the existence of cytotoxicity-associated degranulation of Nef187-203-specific CD4$^+$ T cells in these two HIV-1-infected patients.

DISCUSSION

Previous studies showed that Gag and Nef are immunodominant proteins of HIV-1-specific CD4$^+$ T-cell responses in patients at various stages of an HIV-1 infection. Such studies also

TABLE 1. Detection of Nef187-203-specific CD4$^+$ T cells in chronically HIV-1-infected individuals

Subject	HAART	CD4 count (cells/ml)	Viral load (RNA copies/ml)	Frequency (%) of:		
				CD4$^+$ IFN-γ$^+$[a] cells in:		CD4$^+$ IFN-γ$^+$ CD107a$^+$ cells in ex vivo PBMCs[b]
				Cultured PBMCs	Ex vivo PBMCs	
KI-097	+	322	14,000	0	NT[c]	NT
KI-105	+	485	<50	2.2	0	0
KI-121	−	265	24,000	18.4	0	0
KI-139	+	505	110,000	0	NT	NT
KI-144	+	496	17,000	0	NT	NT
KI-152	+	303	<50	0	NT	NT
KI-154	+	481	7,700	70.3	0.01	70.0
KI-163	+	419	26,000	0	NT	NT
KI-185	+	331	<50	0	NT	NT
KI-197	+	350	<50	60.7	0.06	55.0

[a] IFN-γ$^+$, IFN-γ-producing.
[b] Frequency among Nef187-203-specific CD4$^+$ IFN-γ$^+$ cells.
[c] NT, not tested.

revealed that only a limited number of peptides may induce CD4 T-cell responses in a genetically diverse population (1, 27). In the present study, we found two Nef $CD4^+$ T-cell epitopes, Nef37-53 and Nef187-203, from two HIV-1-seropositive donors. A previous study showed that a group of subjects with CD4 T-cell responses targeted the peptide Nef187-203; however, the MHC-II restriction of it was not reported (27). Here we characterized both Nef epitopes as HLA-DR restricted in our subjects. Classically, HLA class II-restricted epitopes are processed through the exogenous pathway. However, for $CD4^+$ T-cell recognition of virus-infected cells, the endogenous pathway for HLA class II presentation was also identified in some virus infections (20, 33, 35). In our present study, Nef-specific $CD4^+$ T-cell clones recognized the epitope presented in recombinant vaccinia virus-infected or Nef-GFP fusion mRNA-transfected B-LCLs through the endogenous pathway as well as through the classical exogenous pathway in the antigen protein-pulsed B-LCLs. Furthermore, Nef187-203-specific $CD4^+$ CTLs recognized HIV-1-infected macrophages and $CD4^+$ T cells, suggesting that these HIV-1 host cells could present Nef protein to MHC-II molecules through the endogenous pathway during an HIV-1 infection. Thus, we demonstrated for the first time both endogenous and exogenous presentation of an HIV-1 CD4 epitope by HLA class II molecules.

Since previous studies showed that Gag-specific $CD4^+$ T cells exhibit cytotoxic activity (4, 30, 31), here also we investigated if the same mechanism exists for another immunodominant HIV-1 antigen, Nef. Strong cytotoxic activity was found in the Nef187-203-specific clones in our present study. Compared with the noncytotoxic Nef37-53-specific clone, the cytotoxic Nef187-203-specific clone showed higher perforin and granzyme B expression levels. Although Th clones can acquire cytotoxic behavior during in vitro culture (15), ex vivo studies have directly indicated the persistence of HIV-1-specific cytotoxic $CD4^+$ T cells (31). In addition, a significantly higher perforin expression in a $CD4^+$ subset of PBMCs from HIV-1-infected patients was also observed earlier, suggesting a high prevalence of cytotoxic $CD4^+$ T cells during an HIV-1 infection (4). In our present study, it is unlikely that the observed Nef-specific cytolysis was an artifact of prolonged culture, because ex vivo analysis showed that Nef187-203-specific $CD4^+$ T cells from two donors mobilized CD107a after stimulation with Nef187-203 peptide. Our observations on the cytotoxic effector molecule expression of Nef-specific $CD4^+$ CTL clones suggest that these CTLs kill their target cells by a perforin-dependent pathway, just as in the case of the Gag-specific $CD4^+$ CTLs reported previously (31). The perforin expression in HIV-1-specific $CD4^+$ T cells may be controlled by the CD8 responses during an infection, producing cross-regulation between HIV-1-specific $CD4^+$ and $CD8^+$ T-cell responses (47).

Although Gag-specific $CD4^+$ CTLs were demonstrated to be able to suppress HIV-1 replication in a $CD4^+$ T-cell line, MT-2 (31), the ability of HIV-1-specific $CD4^+$ CTLs to kill infected natural target cells and to suppress HIV-1 replication in these cells has not been explored. $CD4^+$ T cells under normal conditions do not express any HLA class II molecules. Naturally, HIV-1 can replicate only in activated $CD4^+$ T cells, which express MHC-II and are susceptible to $CD4^+$ CTL killing (22). However, the question as to whether the levels of HLA class II expression on HIV-1-infected activated T cells are high enough for efficient recognition by $CD4^+$ CTLs remains unresolved. In addition, previous studies revealed differential susceptibility to $CD8^+$ CTL killing between HIV-1-infected macrophages and $CD4^+$ T cells, showing the complexity of CTL killing of natural target cells during an HIV-1 infection (12, 17, 40). Here we demonstrated higher specific lysis of infected macrophages by Nef-specific $CD4^+$ CTLs than of infected $CD4^+$ T cells by these cells. This result implies that HIV-1-infected macrophages can present virus antigen to HLA class II molecules more effectively than HIV-1-infected $CD4^+$ T cells. On the other hand, naturally higher HLA class II expression on macrophages may also contribute to more-efficient killing of them by $CD4^+$ CTLs. We observed significant HLA class II downregulation on HIV-1-infected $CD4^+$ T cells but not on the infected macrophages (data not shown), in line with a previous report indicating that HIV-1 proteins impair HLA class II expression on infected $CD4^+$ T cells (26). These findings, taken together, may explain why Nef-specific $CD4^+$ CTLs killed HIV-1-infected macrophages more efficiently than HIV-1-infected $CD4^+$ T cells.

Although a difference between cytotoxic activity against HIV-1-infected macrophages and that against $CD4^+$ T cells was observed, Nef-specific $CD4^+$ CTL clones exhibited complete suppression of HIV-1 replication in both kinds of host cells, even at an initial E/T ratio of 0.1 in the assay. The Nef187-203-specific $CD4^+$ CTL clones exhibited a more than 10-fold-stronger ability to suppress HIV-1 replication in macrophages or $CD4^+$ T cells than Nef- or Gag-specific $CD8^+$ CTL clones investigated in our previous studies (17, 18), which employed the same assays, suggesting that Nef187-203-specific $CD4^+$ T cells may be capable of suppressing HIV-1 replication in vivo. In principle, HIV-1-specific T-cell clones can suppress virus replication in two ways: by suppressing cytotoxic activity and cytokine production. A recent study showed that in vitro-cultured noncytotoxic $CD4^+$ T cells produced CCR5 chemokines to suppress HIV-1 replication in those cells themselves (28). In our study, the high level of Mip-1β production by Nef187-203-specific $CD4^+$ CTL clones (data not shown) might also have partly contributed to the suppression of virus replication.

Classically, virus-specific $CD4^+$ T cells play a key role in the maintenance of $CD8^+$ CTL memory (24, 42). In the present study, we sought to demonstrate roles of Nef-specific $CD4^+$ CTLs beyond such helper functions. Notably, we found the suppression of HIV-1 replication in host macrophages and $CD4^+$ T cells by Nef-specific $CD4^+$ CTL clones. Previous investigations showed macrophages to be major reservoirs for HIV-1 in an early infection and in patients with an undetectable viral load on HAART (13). Furthermore, HIV-1-infected macrophages mediate infection of nonlymphoid tissues such as lung or brain (43). Therefore, the strong ability of Nef-specific $CD4^+$ CTLs to suppress HIV-1 replication in macrophages might help to control HIV-1 rebound in structured treatment interruption patients and to relieve the neuropathology associated with AIDS. In addition, Nef-specific $CD4^+$ CTLs may target HIV-infected host cells that resist $CD8^+$ CTL recognition due to an impaired HLA class I antigen-processing pathway. Studies on EBV-specific $CD4^+$ CTLs indicated that they killed EBV-positive Burkitt's lymphoma cells, which are resistant to $CD8^+$ CTL killing, through impaired MHC-I antigen

presentation (2, 37). Thus, particularly in the tissues that can express HLA class II molecules, such as dendritic cells, macrophages, and activated T cells, HIV-1-specific $CD4^+$ CTLs may take the position left vacant due to escape from $CD8^+$ CTL surveillance. However, $CD4^+$ CTLs can also target the antigen-presenting cells and bystander $CD4^+$ T cells, which present epitope peptides through the exogenous pathway. As mentioned by Norris et al. (31), this effect may result in depletion of healthy immune cells during an HIV infection. These results, taken together, indicate that the influence of $CD4^+$ CTLs in vivo on the disease development of AIDS requires more consideration. The frequency of HLA-DR0803-positive patients that responded to the Nef187-203 epitope assessed in our study was 40%, although this value probably was underestimated because previous reports showed that some patients might lose CD4 responses specific for HIV-1 antigens due to vigorous HIV-1 reproduction (7). Exact assessment of the frequency of HIV-1-specific $CD4^+$ T cells would require the use of more-sensitive and cytokine/cytotoxicity response-independent techniques, such as those involving MHC-II tetramers (21).

Overall, our results demonstrated that Nef-specific cytotoxic $CD4^+$ T cells killed HIV-1-infected $CD4^+$ T cells and macrophages in a perforin-mediated manner and that the cytotoxic $CD4^+$ T cells exhibited strong ability to suppress HIV-1 replication in the natural host cells. In addition, our ex vivo analysis revealed that these cytotoxic $CD4^+$ T cells could be detected in 20% of the chronically HIV-infected patients tested. These results, taken together, suggest the importance of Nef-specific $CD4^+$ T cells in the control of HIV-1 infections in vivo.

ACKNOWLEDGMENTS

We thank Sachiko Sakai for secretarial assistance.

This research was supported by the Program of Founding Research Centers for Emerging and Reemerging Infectious Diseases and by the Global COE program Global Education and Research Center Aiming at the Control of AIDS, supported by the Ministry of Education, Science, Sports and Culture, Japan; by a grant-in-aid (no. 20390134) for scientific research from the Ministry of Health, Japan; by a grant-in-aid (no. 18390141) for scientific research from the Ministry of Education, Science, Sports and Culture, Japan; and by a grant from the Japan Health Science Foundation.

REFERENCES

1. **Addo, M. M., X. G. Yu, A. Rathod, D. Cohen, R. L. Eldridge, D. Strick, M. N. Johnston, C. Corcoran, A. G. Wurcel, C. A. Fitzpatrick, M. E. Feeney, W. R. Rodriguez, N. Basgoz, R. Draenert, D. R. Stone, C. Brander, P. J. Goulder, E. S. Rosenberg, M. Altfeld, and B. D. Walker.** 2003. Comprehensive epitope analysis of human immunodeficiency virus type 1 (HIV-1)-specific T-cell responses directed against the entire expressed HIV-1 genome demonstrate broadly directed responses, but no correlation to viral load. J. Virol. **77**:2081–2092.
2. **Adhikary, D., U. Behrends, A. Moosmann, K. Witter, G. W. Bornkamm, and J. Mautner.** 2006. Control of Epstein-Barr virus infection in vitro by T helper cells specific for virion glycoproteins. J. Exp. Med. **203**:995–1006.
3. **Appay, V.** 2004. The physiological role of cytotoxic $CD4^+$ T-cells: the holy grail? Clin. Exp. Immunol. **138**:10–13.
4. **Appay, V., J. J. Zaunders, L. Papagno, J. Sutton, A. Jaramillo, A. Waters, P. Easterbrook, P. Grey, D. Smith, A. J. McMichael, D. A. Cooper, S. L. Rowland-Jones, and A. D. Kelleher.** 2002. Characterization of $CD4^+$ CTLs ex vivo. J. Immunol. **168**:5954–5958.
5. **Betts, M. R., D. R. Ambrozak, D. C. Douek, S. Bonhoeffer, J. M. Brenchley, J. P. Casazza, R. A. Koup, and L. J. Picker.** 2001. Analysis of total human immunodeficiency virus (HIV)-specific $CD4^+$ and $CD8^+$ T-cell responses: relationship to viral load in untreated HIV infection. J. Virol. **75**:11983–11991.
6. **Betts, M. R., and R. A. Koup.** 2004. Detection of T-cell degranulation: CD107a and b. Methods Cell Biol. **75**:497–512.
7. **Binley, J. M., D. S. Schiller, G. M. Ortiz, A. Hurley, D. F. Nixon, M. M. Markowitz, and J. P. Moore.** 2000. The relationship between T cell proliferative responses and plasma viremia during treatment of human immunodeficiency virus type 1 infection with combination antiretroviral therapy. J. Infect. Dis. **181**:1249–1263.
8. **Boaz, M. J., A. Waters, S. Murad, P. J. Easterbrook, and A. Vyakarnam.** 2002. Presence of HIV-1 Gag-specific IFN-gamma$^+$IL-2$^+$ and CD28$^+$IL-2$^+$ CD4 T cell responses is associated with nonprogression in HIV-1 infection. J. Immunol. **169**:6376–6385.
9. **Borrow, P., H. Lewicki, X. Wei, M. S. Horwitz, N. Peffer, H. Meyers, J. A. Nelson, J. E. Gairin, B. H. Hahn, M. B. Oldstone, and G. M. Shaw.** 1997. Antiviral pressure exerted by HIV-1-specific cytotoxic T lymphocytes (CTLs) during primary infection demonstrated by rapid selection of CTL escape virus. Nat. Med. **3**:205–211.
10. **Casazza, J. P., M. R. Betts, D. A. Price, M. L. Precopio, L. E. Ruff, J. M. Brenchley, B. J. Hill, M. Roederer, D. C. Douek, and R. A. Koup.** 2006. Acquisition of direct antiviral effector functions by CMV-specific $CD4^+$ T lymphocytes with cellular maturation. J. Exp. Med. **203**:2865–2877.
11. **Champagne, P., G. S. Ogg, A. S. King, C. Knabenhans, K. Ellefsen, M. Nobile, V. Appay, G. P. Rizzardi, S. Fleury, M. Lipp, R. Forster, S. Rowland-Jones, R. P. Sekaly, A. J. McMichael, and G. Pantaleo.** 2001. Skewed maturation of memory HIV-specific CD8 T lymphocytes. Nature **410**:106–111.
12. **Collins, K. L., B. K. Chen, S. A. Kalams, B. D. Walker, and D. Baltimore.** 1998. HIV-1 Nef protein protects infected primary cells against killing by cytotoxic T lymphocytes. Nature **391**:397–401.
13. **Crowe, S. M., and S. Sonza.** 2000. HIV-1 can be recovered from a variety of cells including peripheral blood monocytes of patients receiving highly active antiretroviral therapy: a further obstacle to eradication. J. Leukoc. Biol. **68**:345–350.
14. **Delmas, S., P. Brousset, D. Clement, E. Le Roy, and J. L. Davignon.** 2007. Anti-IE1 $CD4^+$ T-cell clones kill peptide-pulsed, but not human cytomegalovirus-infected, target cells. J. Gen. Virol. **88**:2441–2449.
15. **Fleischer, B.** 1984. Acquisition of specific cytotoxic activity by human $T4^+$ T lymphocytes in culture. Nature **308**:365–367.
16. **Fujiwara, M., H. Takata, S. Oka, H. Tomiyama, and M. Takiguchi.** 2005. Patterns of cytokine production in human immunodeficiency virus type 1 (HIV-1)-specific human $CD8^+$ T cells after stimulation with HIV-1-infected $CD4^+$ T cells. J. Virol. **79**:12536–12543.
17. **Fujiwara, M., and M. Takiguchi.** 2007. HIV-1-specific CTLs effectively suppress replication of HIV-1 in HIV-1-infected macrophages. Blood **109**:4832–4838.
18. **Fujiwara, M., J. Tanuma, H. Koizumi, Y. Kawashima, K. Honda, S. Mastuoka-Aizawa, S. Dohki, S. Oka, and M. Takiguchi.** 2008. Different abilities of escape mutant-specific cytotoxic T cells to suppress replication of escape mutant and wild-type human immunodeficiency virus type 1 in new hosts. J. Virol. **82**:138–147.
19. **Green, S., I. Kurane, S. Pincus, E. Paoletti, and F. A. Ennis.** 1997. Recognition of dengue virus NS1-NS2a proteins by human $CD4^+$ cytotoxic T lymphocyte clones. Virology **234**:383–386.
20. **Hegde, N. R., C. Dunn, D. M. Lewinsohn, M. A. Jarvis, J. A. Nelson, and D. C. Johnson.** 2005. Endogenous human cytomegalovirus gB is presented efficiently by MHC class II molecules to $CD4^+$ CTL. J. Exp. Med. **202**:1109–1119.
21. **Hohn, H., C. Kortsik, I. Zehbe, W. E. Hitzler, K. Kayser, K. Freitag, C. Neukirch, P. Andersen, T. M. Doherty, and M. Maeurer.** 2007. MHC class II tetramer guided detection of *Mycobacterium tuberculosis*-specific $CD4^+$ T cells in peripheral blood from patients with pulmonary tuberculosis. Scand. J. Immunol. **65**:467–478.
22. **Holling, T. M., N. van der Stoep, E. Quinten, and P. J. van den Elsen.** 2002. Activated human T cells accomplish MHC class II expression through T cell-specific occupation of class II transactivator promoter III. J. Immunol. **168**:763–770.
23. **Jansen, C. A., D. van Baarle, and F. Miedema.** 2006. HIV-specific $CD4^+$ T cells and viremia: who's in control? Trends Immunol. **27**:119–124.
24. **Janssen, E. M., E. E. Lemmens, T. Wolfe, U. Christen, M. G. von Herrath, and S. P. Schoenberger.** 2003. $CD4^+$ T cells are required for secondary expansion and memory in $CD8^+$ T lymphocytes. Nature **421**:852–856.
25. **Jellison, E. R., S. K. Kim, and R. M. Welsh.** 2005. Cutting edge: MHC class II-restricted killing in vivo during viral infection. J. Immunol. **174**:614–618.
26. **Kanazawa, S., T. Okamoto, and B. M. Peterlin.** 2000. Tat competes with CIITA for the binding to P-TEFb and blocks the expression of MHC class II genes in HIV infection. Immunity **12**:61–70.
27. **Kaufmann, D. E., P. M. Bailey, J. Sidney, B. Wagner, P. J. Norris, M. N. Johnston, L. A. Cosimi, M. M. Addo, M. Lichterfeld, M. Altfeld, N. Frahm, C. Brander, A. Sette, B. D. Walker, and E. S. Rosenberg.** 2004. Comprehensive analysis of human immunodeficiency virus type 1-specific CD4 responses reveals marked immunodominance of Gag and Nef and the presence of broadly recognized peptides. J. Virol. **78**:4463–4477.
28. **Kaur, G., M. Tuen, D. Virland, S. Cohen, N. K. Mehra, C. Munz, S. Abdelwahab, A. Garzino-Demo, and C. E. Hioe.** 2007. Antigen stimulation induces HIV envelope gp120-specific $CD4^+$ T cells to secrete CCR5 ligands and suppress HIV infection. Virology **369**:214–225.

29. **Koup, R. A., J. T. Safrit, Y. Cao, C. A. Andrews, G. McLeod, W. Borkowsky, C. Farthing, and D. D. Ho.** 1994. Temporal association of cellular immune responses with the initial control of viremia in primary human immunodeficiency virus type 1 syndrome. J. Virol. **68**:4650–4655.
30. **Lotti, B., T. Wendland, H. Furrer, N. Yawalkar, S. von Greyerz, K. Schnyder, M. Brandes, P. Vernazza, R. Wagner, T. Nguyen, E. Rosenberg, W. J. Pichler, and C. Brander.** 2002. Cytotoxic HIV-1 p55gag-specific CD4+ T cells produce HIV-inhibitory cytokines and chemokines. J. Clin. Immunol. **22**:253–262.
31. **Norris, P. J., H. F. Moffett, O. O. Yang, D. E. Kaufmann, M. J. Clark, M. M. Addo, and E. S. Rosenberg.** 2004. Beyond help: direct effector functions of human immunodeficiency virus type 1-specific CD4+ T cells. J. Virol. **78**: 8844–8851.
32. **Norris, P. J., M. Sumaroka, C. Brander, H. F. Moffett, S. L. Boswell, T. Nguyen, Y. Sykulev, B. D. Walker, and E. S. Rosenberg.** 2001. Multiple effector functions mediated by human immunodeficiency virus-specific CD4+ T-cell clones. J. Virol. **75**:9771–9779.
33. **Nuchtern, J. G., W. E. Biddison, and R. D. Klausner.** 1990. Class II MHC molecules can use the endogenous pathway of antigen presentation. Nature **343**:74–76.
34. **Ogg, G. S., X. Jin, S. Bonhoeffer, P. R. Dunbar, M. A. Nowak, S. Monard, J. P. Segal, Y. Cao, S. L. Rowland-Jones, V. Cerundolo, A. Hurley, M. Markowitz, D. D. Ho, D. F. Nixon, and A. J. McMichael.** 1998. Quantitation of HIV-1-specific cytotoxic T lymphocytes and plasma load of viral RNA. Science **279**:2103–2106.
35. **Orentas, R. J., J. E. Hildreth, E. Obah, M. Polydefkis, G. E. Smith, M. L. Clements, and R. F. Siliciano.** 1990. Induction of CD4+ human cytolytic T cells specific for HIV-infected cells by a gp160 subunit vaccine. Science **248**:1234–1237.
36. **Palmer, B. E., E. Boritz, and C. C. Wilson.** 2004. Effects of sustained HIV-1 plasma viremia on HIV-1 Gag-specific CD4+ T cell maturation and function. J. Immunol. **172**:3337–3347.
37. **Paludan, C., K. Bickham, S. Nikiforow, M. L. Tsang, K. Goodman, W. A. Hanekom, J. F. Fonteneau, S. Stevanovic, and C. Munz.** 2002. Epstein-Barr nuclear antigen 1-specific CD4+ Th1 cells kill Burkitt's lymphoma cells. J. Immunol. **169**:1593–1603.
38. **Penna, A., P. Fowler, A. Bertoletti, S. Guilhot, B. Moss, R. F. Margolskee, A. Cavalli, A. Valli, F. Fiaccadori, F. V. Chisari, et al.** 1992. Hepatitis B virus (HBV)-specific cytotoxic T-cell (CTL) response in humans: characterization of HLA class II-restricted CTLs that recognize endogenously synthesized HBV envelope antigens. J. Virol. **66**:1193–1198.
39. **Pitcher, C. J., C. Quittner, D. M. Peterson, M. Connors, R. A. Koup, V. C. Maino, and L. J. Picker.** 1999. HIV-1-specific CD4+ T cells are detectable in most individuals with active HIV-1 infection, but decline with prolonged viral suppression. Nat. Med. **5**:518–525.
40. **Plata, F., B. Autran, L. P. Martins, S. Wain-Hobson, M. Raphael, C. Mayaud, M. Denis, J. M. Guillon, and P. Debre.** 1987. AIDS virus-specific cytotoxic T lymphocytes in lung disorders. Nature **328**:348–351.
41. **Rosenberg, E. S., J. M. Billingsley, A. M. Caliendo, S. L. Boswell, P. E. Sax, S. A. Kalams, and B. D. Walker.** 1997. Vigorous HIV-1-specific CD4+ T cell responses associated with control of viremia. Science **278**:1447–1450.
42. **Shedlock, D. J., and H. Shen.** 2003. Requirement for CD4 T cell help in generating functional CD8 T cell memory. Science **300**:337–339.
43. **Stevenson, M.** 2003. HIV-1 pathogenesis. Nat. Med. **9**:853–860.
44. **Takata, H., and M. Takiguchi.** 2006. Three memory subsets of human CD8+ T cells differently expressing three cytolytic effector molecules. J. Immunol. **177**:4330–4340.
45. **Tomiyama, H., H. Akari, A. Adachi, and M. Takiguchi.** 2002. Different effects of Nef-mediated HLA class I down-regulation on human immunodeficiency virus type 1-specific CD8+ T-cell cytolytic activity and cytokine production. J. Virol. **76**:7535–7543.
46. **Ueno, T., Y. Idegami, C. Motozono, S. Oka, and M. Takiguchi.** 2007. Altering effects of antigenic variations in HIV-1 on antiviral effectiveness of HIV-specific CTLs. J. Immunol. **178**:5513–5523.
47. **Williams, N. S., and V. H. Engelhard.** 1997. Perforin-dependent cytotoxic activity and lymphokine secretion by CD4+ T cells are regulated by CD8+ T cells. J. Immunol. **159**:2091–2099.
48. **Wilson, J. D., N. Imami, A. Watkins, J. Gill, P. Hay, B. Gazzard, M. Westby, and F. M. Gotch.** 2000. Loss of CD4+ T cell proliferative ability but not loss of human immunodeficiency virus type 1 specificity equates with progression to disease. J. Infect. Dis. **182**:792–798.
49. **Xu, X. N., G. R. Screaton, F. M. Gotch, T. Dong, R. Tan, N. Almond, B. Walker, R. Stebbings, K. Kent, S. Nagata, J. E. Stott, and A. J. McMichael.** 1997. Evasion of cytotoxic T lymphocyte (CTL) responses by nef-dependent induction of Fas ligand (CD95L) expression on simian immunodeficiency virus-infected cells. J. Exp. Med. **186**:7–16.
50. **Zaunders, J. J., W. B. Dyer, B. Wang, M. L. Munier, M. Miranda-Saksena, R. Newton, J. Moore, C. R. Mackay, D. A. Cooper, N. K. Saksena, and A. D. Kelleher.** 2004. Identification of circulating antigen-specific CD4+ T lymphocytes with a CCR5+, cytotoxic phenotype in an HIV-1 long-term nonprogressor and in CMV infection. Blood **103**:2238–2247.

Journal of Cellular Physiology

Dys-Regulated Activation of a Src Tyroine Kinase Hck at the Golgi Disturbs *N*-Glycosylation of a Cytokine Receptor Fms

RANYA HASSAN,[1] SHINYA SUZU,[1] MASATERU HIYOSHI,[1] NAOKO TAKAHASHI-MAKISE,[1] TAKAMASA UENO,[2] TSUTOMU AGATSUMA,[3] HIROFUMI AKARI,[4] JUN KOMANO,[5] YUTAKA TAKEBE,[6] KAZUO MOTOYOSHI,[7] AND SEIJI OKADA[1]*

[1]*Division of Hematopoiesis, Center for AIDS Research, Kumamoto University, Kumamoto, Kumamoto, Japan*

[2]*Viral Immunology, Center for AIDS Research, Kumamoto University, Kumamoto, Kumamoto, Japan*

[3]*Tokyo Research Laboratories, Kyowa Hakko Co., Ltd, Machida, Tokyo, Japan*

[4]*Laboratory of Disease Control, Tsukuba Primate Research Center, National Institute of Biomedical Innovation, Tsukuba, Ibaraki, Japan*

[5]*Laboratory of Virology and Pathogenesis, AIDS Research Center, National Institute of Infectious Diseases, Shinjuku, Tokyo, Japan*

[6]*Laboratory of Molecular Biology and Epidemiology, AIDS Research Center, National Institute of Infectious Diseases, Shinjuku, Tokyo, Japan*

[7]*Department of Internal Medicine, National Defense Medical College, Tokorozawa, Saitama, Japan*

HIV-1 Nef accelerates the progression to AIDS by binding with and activating a Src kinase Hck, but underlying molecular basis is not understood. We revealed that Nef disturbed *N*-glycosylation/trafficking of a cytokine receptor Fms in an Hck-dependent manner, a possible trigger to worsen uncontrolled immune system. Here, we provide direct evidence that dys-regulated activation of Hck pre-localized to the Golgi apparatus causes this Fms maturation arrest. A striking change in Hck induced by Nef other than activation was its skewed localization to the Golgi due to predominant Golgi-localization of Nef. Studies with different Nef alleles and their mutants showed a clear correlation among higher Nef-Hck affinity, stronger Hck activation, severe Golgi-localization of Hck and severe Fms maturation arrest. Studies with a newly discovered Nef-Hck binding blocker 2c more clearly showed that skewed Golgi-localization of active Hck was indeed the cause of Fms maturation arrest. 2c blocked Nef-induced skewed Golgi-localization of an active form of Hck (Hck-P2A) and Fms maturation arrest by Nef/Hck-P2A, but showed no inhibition on Hck-P2A kinase activity. Our finding establishes an intriguing link between the pathogenesis of Nef and a newly emerging concept that the Golgi-localized Src kinases regulate the Golgi function.

J. Cell. Physiol. 221: 458–468, 2009.

Studies of HIV-1-infected patients and monkey models have demonstrated that Nef, a protein with no enzymatic activity encoded by the HIV-1 genome, is a critical determinant for the development of AIDS (Kestler et al., 1991; Deacon et al., 1995; Kirchhoff et al., 1995). Subsequent studies of HIV-1 transgenic (Tg) mice supported the idea. The expression of entire coding sequences of HIV-1 in $CD4^+$ T cells and macrophages caused an AIDS-like disease, which was abolished by Nef deletion (Hanna et al., 1998). This pathogenetic activity of Nef is supposed to be mediated by its binding with cellular proteins, and a well-defined partner of Nef is Hck (Saksela et al., 1995), a member of Src family tyrosine kinases expressed in macrophages. Other Src kinases (Lyn, Fyn, c-Src, and Lck) bind Nef but with lower affinities (Arold et al., 1998; Karkkainen et al., 2006; Trible et al., 2006). Importantly, the disruption of proline-rich PxxP motif of Nef, an essential motif to bind the Src homology 3 (SH3) domain of Hck, was sufficient to protect Tg mice from the AIDS-like disease, and wild-type Nef-induced disease progression was significantly delayed in $Hck^{-/-}$ mice (Hanna et al., 2001), indicating that high affinity Nef-Hck binding in macrophages is at least in part responsible for disease development and progression. However, unresolved issue is how Nef-Hck binding followed by activation of Hck (Moarefi et al., 1997; Lerner and Smithgall, 2002) satisfactorily account for disease development and progression.

An important clue to the issue is that Nef predominantly localized to the Golgi apparatus (Greenberg et al., 1998; Drakesmith et al., 2005; Haller et al., 2007) and that Nef not only activated Hck but also induced skewed localization of Hck to the Golgi (Hung et al., 2007). The Golgi functions as a sorting hub and location of glycosylation for proteins, and several lines of evidence have revealed that Src kinases, shown to be involved in a wide array of intracellular signaling (reviewed in

Contract grant sponsor: Ministry of Education, Culture, Sports, Science and Technology of Japan.
Contract grant sponsor: Human Science Foundation, Japan.

*Correspondence to: Seiji Okada, Division of Hematopoiesis, Center for AIDS Research, Kumamoto University, Kumamoto 860-0811, Japan. E-mail: okadas@kumamoto-u.ac.jp

Received 17 February 2009; Accepted 11 June 2009

Published online in Wiley InterScience (www.interscience.wiley.com.), 7 July 2009.
DOI: 10.1002/jcp.21878

Lowell, 2004), also play a role in the regulation of the Golgi structure/function. First, a fraction of Src kinases, including Hck, is physiologically found at the Golgi (David-Pfeuty and Nouvian-Dooghe, 1990; Kaplan et al., 1992; Ley et al., 1994; Bijlmakers et al., 1997; van't Hof and Resh, 1997; Carreno et al., 2000; Kasahara et al., 2004). Second, fibroblasts lacking three ubiquitous Src kinases (c-Src/Yes/Fyn) exhibited an aberrant Golgi structure composed of collapsed stacks and bloated cisternae (Bard et al., 2003). Third, an increased protein load entering the *cis*-Golgi from the endoplasmic reticulum activated the Golgi-localized Src kinases, which in turn regulated overall protein trafficking activity in the secretory pathway (Pulvirenti et al., 2008). Importantly, the study by Pulvirenti et al. indicates that coordinated regulation of activity of the Golgi-localized Src kinases is crucial to maintain the Golgi function, which raises an intriguing possibility that Nef affects protein trafficking process and thereby macrophage phenotype/function through skewed Golgi-localization of active Hck.

Indeed, we recently identified an aberrant function of Nef, which was possibly due to the skewed Golgi-localization of active Hck. We previously found that Nef inhibited the signal of M-CSF, a primary cytokine for macrophages (Suzu et al., 2005), which was a possible trigger to worsen uncontrolled immune systems in patients, as M-CSF is essential to maintain macrophages at an anti-inflammatory state (reviewed in Hamilton, 2008). Of interest was the role of Hck in this inhibitory activity of Nef (Hiyoshi et al., 2008). Nef reduced cell surface expression of M-CSF receptor Fms in myeloid cells and macrophages, which was the direct cause of the inhibitory activity of Nef on M-CSF signal. Importantly, such reduced cell surface expression of Fms was reproduced in transfected 293 cells, but only in co-expression with Hck. More importantly, the reduced cell surface expression was due to the accumulation of an immature under-*N*-glycosylated Fms at the Golgi (hereinafter called Fms maturation arrest). However, constitutive-active Hck alone failed to induce such Fms maturation arrest. These results indicate that Nef inhibits M-CSF signal by arresting Fms *N*-glycosylation and trafficking at the Golgi and that such Fms maturation arrest was not caused just because of Hck activation. Thus, a most likely cause of Nef-induced Fms maturation arrest was skewed Golgi-localization of active Hck. However, this intriguing hypothesis should be carefully and directly tested, because it will not only help to clarify molecular basis of this novel function of Nef through Hck, but also provide an excellent example of disease-associated failure of the Golgi function regulation by the Golgi-localized Src kinases.

In this study, we therefore sought to definitely conclude that skewed Golgi-localization of active Hck was indeed the direct cause of Fms maturation arrest by Nef. To this end, we employed two different approaches. First, we prepared various Nef proteins and compared their abilities to induce skewed Golgi-localization of Hck, Hck activation and Fms maturation arrest. Second and importantly, we discovered a small-molecule non-kinase inhibitor that effectively blocked Nef-Hck binding and performed mechanistic analyses with the newly discovered compound.

Materials and Methods

Expression plasmids

For the expression in HEK293 cells (Invitrogen, Carlsbad, CA), human Fms- and human p56Hck cDNA cloned into pCDNA3.1 vector (Invitrogen) were used (Suzu et al., 2005; Hiyoshi et al., 2008). The constitutive-active Hck P2A mutant (Hiyoshi et al., 2008) was also used in selected experiments. The expression plasmid for human Lyn cloned in pME-puro vector was provided by Y. Yamanashi (Tokyo Medical and Dental University, Tokyo, Japan) and used in the pull-down assay with GST-Nef fusion proteins (see below). Nef cDNA derived from the NL43 or SF2 strain of HIV-1 was cloned into pRc/CMV-CD8 vector to express the extracellular/transmembrane regions of CD8-Nef fusion protein (Hiyoshi et al., 2008). NL43 Nef-M20A was prepared as described previously (Akari et al., 2000). NL43 Nef-AxxA and $-\Delta E$ mutant were provided by A. Adachi (University of Tokushima, Tokushima, Japan) and J.C. Guatelli (University of California, San Diego, CA), respectively. In this study, we prepared another NL43 Nef mutant (NL43 Nef-TR), by using QuikChange II Site-directed Mutagenesis Kits (Stratagene, La Jolla, CA). We also prepared Nef constructs expressing Nef-GFP fusion proteins (Ueno et al., 2008). For the expression of GST-Nef fusion proteins, fragments containing the entire coding sequences of the wild-type NL43 Nef, NL43 Nef-TR mutant, wild-type SF2 Nef, and SF2 Nef-AxxA mutant were subcloned into pGEX-6P-1 vector (GE Healthcare, Buckinghamshire, UK). SF2 Nef-AxxA mutant was prepared by using QuikChange II Site-directed Mutagenesis Kits (Stratagene). The nucleotide sequences of the coding region of all Nef constructs were verified by using BigDye Terminator v3.1 Cycle Sequencing Kit (Applied Biosystems, Foster City, CA) and ABI PRISM 3100 Genetic Analyzer (Applied Biosystems).

Chemicals

PP2 (Sigma, San Diego, CA) was used as the Src kinase inhibitor. UCS15A and its synthetic derivatives, 2b and 2c, were prepared as described (Oneyama et al., 2003). All these inhibitors were dissolved in dimethyl sulfoxide (DMSO; Wako, Osaka, Japan).

Western blotting

HEK293 cells were maintained with DME medium (Wako) supplemented with 10% fetal calf serum (FCS). The maturation of Fms proteins or the activation of Hck was analyzed by the transient expression assay with the cells followed by Western blotting as described previously (Suzu et al., 2005; Hiyoshi et al., 2008). In brief, cells grown on a 12-well tissue culture plate were transfected with plasmid for Fms (0.4 μg), Nef (0.8 μg), or Hck (0.4 μg) in the combinations indicated using LipofectAMINE2000 reagent (Invitrogen), unless otherwise stated. Total amounts of plasmids were normalized with the empty vectors. After 6 h, culture medium was replaced with complete medium and the transfected cells were cultured for an additional 42 h. In selected experiments, chemicals such as PP2 and 2c were added to the culture at the same time of changing medium. Total cell lysates were prepared essentially as described (Suzu et al., 2000). Primary antibodies used for Western blotting were as follows: anti-Fms (C-20; Santa Cruz Biotechnology, Santa Cruz, CA), anti-CD8 (H-160; Santa Cruz), anti-GFP (FL; Santa Cruz), anti-Hck (clone 18; Transduction Laboratories, Lexington, KY), anti-Hck phosphorylated at tyrosine 411 (Hck-pTyr^{411}; Santa Cruz), anti-phosphotyrosine (PY99; Santa Cruz), and anti-ERK1/2 (K-23; Santa Cruz). The relative intensity of bands on scanned gel images was quantified using NIH Image software, and the Fms maturation arrest or Hck activation is also shown graphically on an arbitrary unit. The relative intensity of bands on Hck-pTyr^{411} blots was quantified and the degree of Hck activation was expressed as a fold-increase relative to the control. For Fms maturation arrest, we calculated the percentage of immature under-*N*-glycosylated Fms of total Fms protein amount, and compared the percentages among samples.

Immunofluorescence

The signal of Nef-GFP was directly visualized with a BZ-8000 fluorescent microscope (Keyence, Osaka, Japan) equipped with Plan-Fluor ELWD 20x/0.45 objective lenses (Nikon, Tokyo, Japan) (Hiyoshi et al., 2008). To detect active Hck, cells were fixed in 2% paraformaldehyde, permeabilized with ethanol, and stained with goat anti-active Hck antibodies (Santa Cruz). Secondary antibodies were anti-goat IgG-AlexaFluo488 (Molecular Probes, Eugene, OR). Nuclei were stained with DAPI (Molecular Probes), and

fluorescent signals were visualized as above. Image processing was performed using BZ-analyzer (Keyence) and Adobe Photoshop Software (Adobe Systems, San Jose, CA).

GST pull-down

The control GST or GST-Nef fusion proteins (wild-type NL43 Nef, NL43 Nef-TR, wild-type SF2 Nef, and SF2 Nef-AxxA) cloned in pGEX-6P-1 vector was expressed in *E. coli* BL21 cells (GE Healthcare). Cells were grown in LB media containing 50 μg/ml ampicillin followed by induction with 1 μM IPTG. The expression-induced cells were harvested and lysed with BugBuster Protein Extraction Reagent containing 1 U/ml rLysozyme and 25 U/ml Benzonaze Nuclease (Novagen, Madison, WI). The cleared lysates were then incubated with GST-Bind Resin (Novagen). After extensive washing with GST Bind/Wash Buffer (Novagen), the resin was incubated with the total cell lysates of HEK293 cells transfected with the expression plasmid for Hck or Lyn. In a selected experiment, 2c was added to the mixtures. After extensive re-washing, the resin was boiled with SDS–PAGE sample buffer and elutes were analyzed for the presence of Hck or Lyn by western blotting. Primary antibodies used were as follows (both from Transduction Laboratories): anti-Hck (clone 18) and anti-Lyn (clone 42). In a selected experiment, we also used GST proteins fused to the SH3 domain of Hck (Paliwal et al., 2007), which was provided by G. Swarup (Center for Cellular and Molecular Biology, Hyderabad, India).

Subcellular fractionation

The subcellular fractionation on sucrose gradients was performed exactly as reported (Matsuda et al., 2006). In brief, cells were

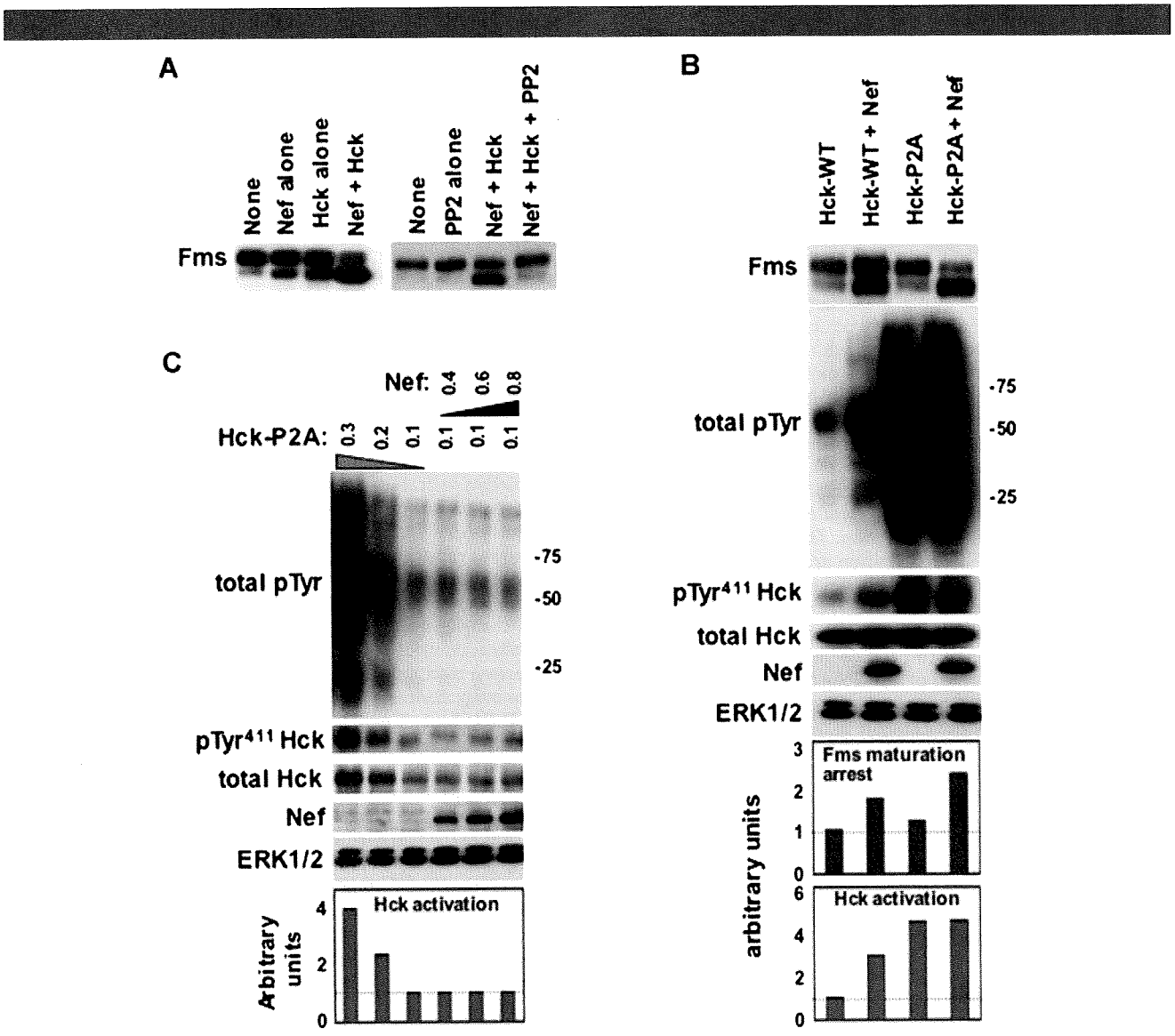

Fig. 1. Nef/Hck-induced Fms mturation arrest. A: HEK293 cells were transfected with Fms plamid alone (None) or co-transfected with the plasmids for NL43 Nef and/or wild-type Hck as indicated. In the right blot, PP2 was added to selected wells at a final concentration of 10 μM after the transfection, Total cell lysates were subjected to Fms Western blotting. B: Cells were transfected with Fms plasmid alone (None) or in combination with the plasmids for Nef (NL43) and Hck (WT or constitutive-active P2A), as indicated. These cells were then analyzed for the expression of Fms, tyrosine-phosphorylated proteins (total pTyr), active-Hck (pTyr^{411}Hck), total Hck, CD8-Nef (Nef), or ERK by Western blotting. The ERK blot is a loading control. The quantified Fms maturation arrest and Hck activation are shown in the bar graphs. C: Cells were transfected with varying amounts (μg) of Hck-P2A and NL43 Nef plasmids as indicated, and analyzed as in (B). The quantified Hck activation is shown in the bar graphs. [Color figure can be viewed in the online issue, which is available at www.interscience.wiley.com.]

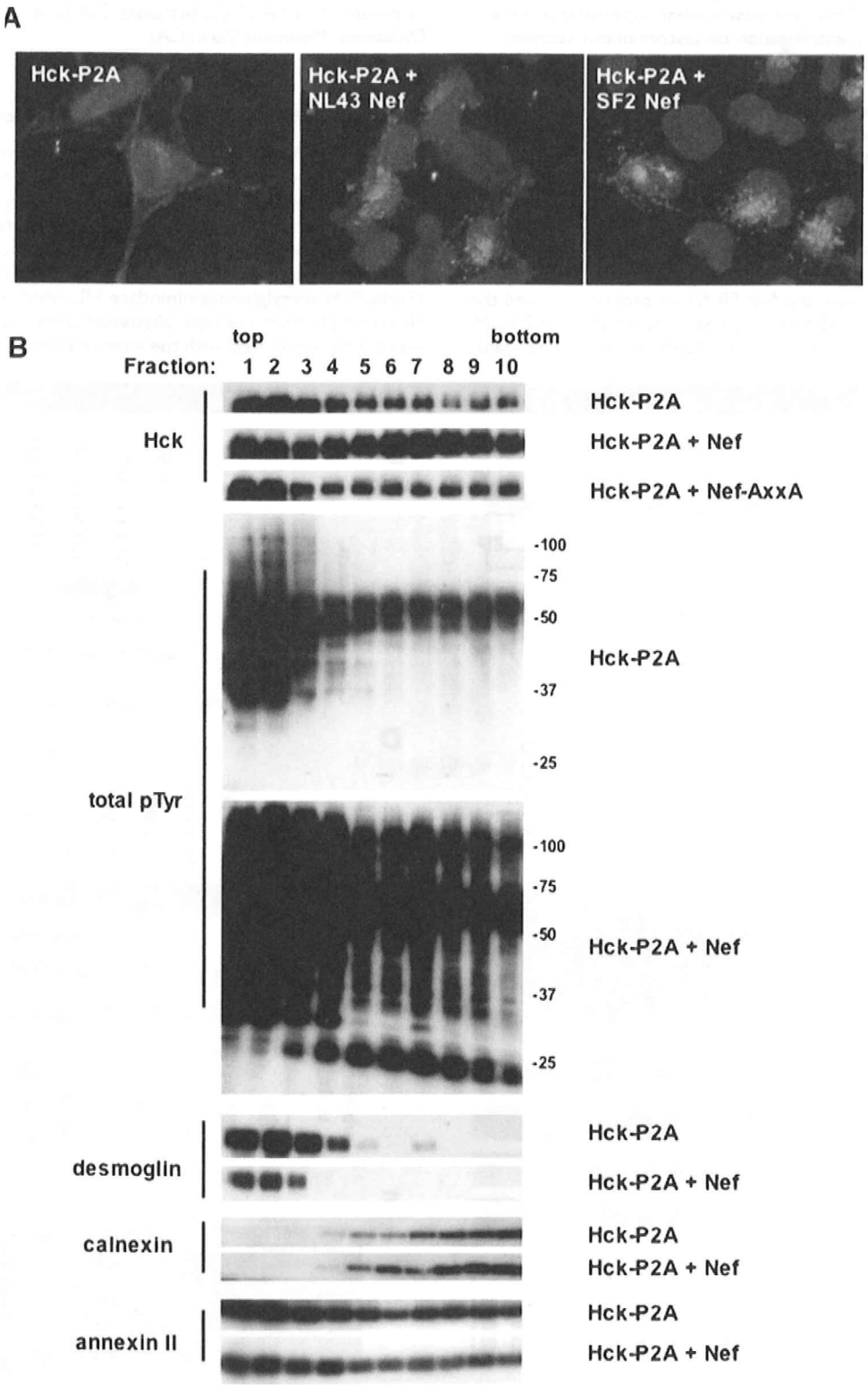

Fig. 2. Skewed Golgi-localization of Hck by Nef. A: HEK293 cells were transfected with Hck-P2A plasmid alone, or co-transfected with NL43 Nef or SF2 Nef plasmid. Cells were stained with antibody specific for active Hck (green) and DAPI (blue). B: Cells were transfected with Hck-P2A alone, or co-transfected with NL43 Nef. Then, cells were subjected to subcellular fractionation on sucrose gradients and Western blotting with antibodies against Hck, phosphotyrosine (pTyr), desmoglein, calnexin, or annexin II. [Color figure can be viewed in the online issue, which is available at www.interscience.wiley.com.]

swollen in hypotonic buffer containing protease inhibitors followed by homogenization. Then, the post-nuclear supernatants were fractionated by ultracentrifugation on discontinuous sucrose gradients. All steps were carried out on ice. The fractions obtained were subjected to Western blotting with antibodies to Hck (clone 18; Transduction Laboratories), desmoglein (clone 62; Transduction Laboratories), annexin II (C-10; Santa Cruz), or calnexin (H-70; Santa Cruz).

Flow cytometry

Human myeloid TF-1-fms cells expressing Nef-ER fusion protein were maintained as described previously (Suzu et al., 2005; Hiyoshi et al., 2008). To activate the Nef-ER fusion protein, we used the estrogen analog 4-HT (Sigma) at a final concentration of 0.1 μM. The cells were stained with PE-labeled anti-Fms antibodies (Santa Cruz), and the level of cell surface Fms was analyzed by flow cytometry on a FACS Calibur using Cell Quest software (Becton Dickinson, Mountain View, CA).

Results

Analyses with Src kinase inhibitor and Hck mutant

As reported, Nef induces Fms maturation arrest when co-expressed with Hck in HEK293 cells (Fig. 1A). HEK293 cells do not express Hck endogenously, and the upper and lower band was the fully *N*-glycosylated and under-*N*-glycosylated Fms, respectively (Hiyoshi et al., 2008). The low molecular weight Fms was sensitive to Endo-H (Endo-β-*N*-acetylglucosaminindase H), which selectively cleaves high-mannose type oligosaccharide, and their increase was clearly associated with the intense staining of Fms mainly at

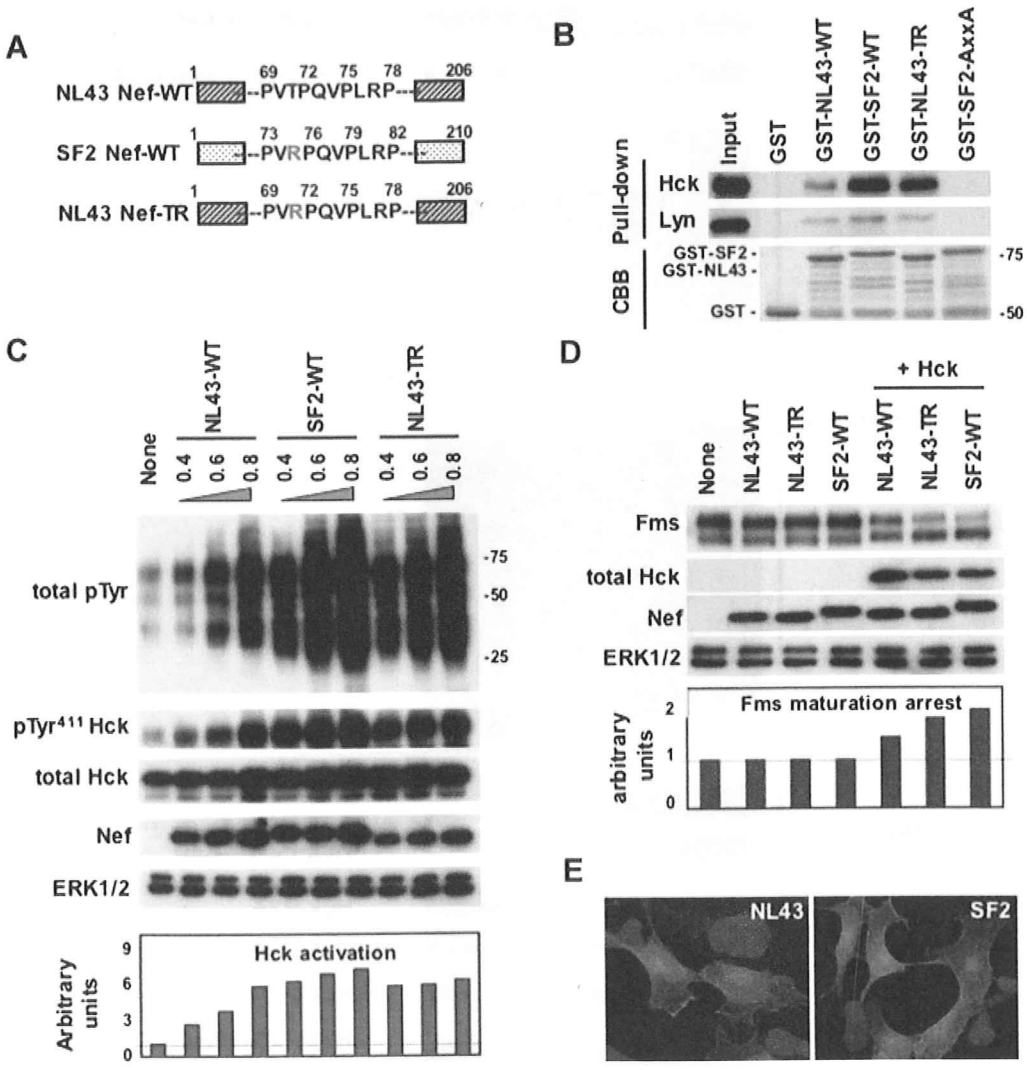

Fig. 3. Abilities of different Nef alleles to bind/activate Hck and to induce Fms maturation arrest. A: The NL43 Nef, SF2 Nef, and NL43 Nef-TR mutant used are schematically shown. B: The resins, to which the control GST or indicated GST-Nef proteins were bound, were incubated with the lysates of HEK293 cells expressing Hck or Lyn. The amount of Hck or Lyn bound to the resins was determined by Western blotting (Pull-down). The amount of GST and GST-Nef fusion proteins bound to the resins was verified by the elution from the resins followed by SDS–PAGE/Coomassie brilliant blue (CBB) staining. C: HEK293 cells were co-transfected with the wild-type Hck and indicated Nef alleles. The amounts of Nef plasmids used are shown (0.4, 0.6, or 0.8 μg/well). Total cell lysates were subjected to Western blotting with antibodies against phosphotyrosine (total pTyr), active-Hck (pTyr^{411}Hck), total Hck, CD8-Nef (Nef), or ERK by Western blotting. The quantified Hck activation is shown in the bar graph. D: Cells were transfected with Fms plasmid alone (None) or in combination with the plasmids for Nef and Hck, as indicated. Western blotting was done as in (C). E: Cells were transfected with indicated GFP-Nef plasmid (green). Nuclei were stained with DAPI (blue). [Color figure can be viewed in the online issue, which is available at www.interscience.wiley.com.]

the perinuclear region, which overlapped well with the signal of GM130 or Vti1a, the markers for the Golgi (Hiyoshi et al., 2008). These results strongly suggested that the low molecular weight Fms was the immature under-*N*-glycosylated form. The increase of the lower molecular weight species was obvious in the cells co-expressing Nef and Hck (Fig. 1A, left blot), and this Fms maturation arrest was blocked by a Src kinase inhibitor PP2 (Fig. 1A, right blot). However, the expression of a constitutive-active Hck mutant (Hck-P2A; Lerner and Smithgall, 2002) was not sufficient to induce Fms maturation arrest when expressed alone (Fig. 1B, Fms blot), despite its strong kinase activity (total pTyr and $pTyr^{411}$ Hck blots). In this study, we monitored kinase activity of Hck by overall protein tyrosine-phosphorylation (total pTyr) and auto-phosphorylation of Hck ($pTyr^{411}$ Hck) (reviewed in Korade-Mirnics and Corey, 2000). Nonetheless, Hck-P2A/Nef co-expression induced more severe Fms maturation arrest than wild-type Hck/Nef co-expression (Fig. 1B), and Nef did not enhance the kinase activity of Hck-P2A (Fig. 1C), confirming our previous finding that Hck activation was necessary but not sufficient for Nef-induced Fms maturation arrest.

Analyses with different Nef alleles and their mutants

In this study, we first found that Nef derived from SF2 strain of HIV-1 induced more severe Golgi-localization of Hck-P2A than Nef derived from NL43 strain. Hck-P2A signal at the plasma membrane was still observed in some NL43 Nef-transfected cells, whereas such signal was not observed in SF2 Nef-transfected cells (Fig. 2A). The Nef-induced skewed Golgi-localization of Hck-2PA was confirmed by a quantitative analysis, that is, subcellular fractionation on sucrose gradients. Based on a previous report (Matsuda et al., 2006), we used desmoglein, annexin II and calnexin as marker proteins for the plasma membrane, both the plasma membrane and the Golgi, and the endoplasmic reticulum, respectively. As shown (Fig. 2B), the plasma membrane was recovered in light fractions whereas the Golgi and the endoplasmic reticulum were recovered in heavy fractions, and the peak of Hck-P2A shifted to heavy fractions by the co-expression with NL43 Nef but not a Nef-AxxA mutant defective in the binding to Hck (Saksela et al., 1995). The peak shift was also associated with the appearance of many tyrosine-phosphorylated proteins in these fractions (Fig. 2B).

Both NL43 Nef and SF2 Nef had intact PxxP motif (Fig. 3A), but SF2 Nef showed much higher affinity to Hck than NL43 Nef (Fig. 3B). In the control experiments, we confirmed that the binding of both Nef to Lyn remained low and the PxxP motif-disrupted SF2 Nef mutant (AxxA) bound neither Hck nor Lyn. Reflecting the higher affinity to Hck, SF2 Nef induced stronger Hck activation (Fig. 3C) and more severe Fms maturation arrest (Fig. 3D). As expected, even SF2 Nef failed to induce Fms maturation arrest when co-expressed with Lyn (data not shown). However, SF2 Nef and NL43 Nef showed no obvious change in the pattern of predominant Golgi-localization (Fig. 3E). It was therefore likely that SF2 Nef bound Hck at

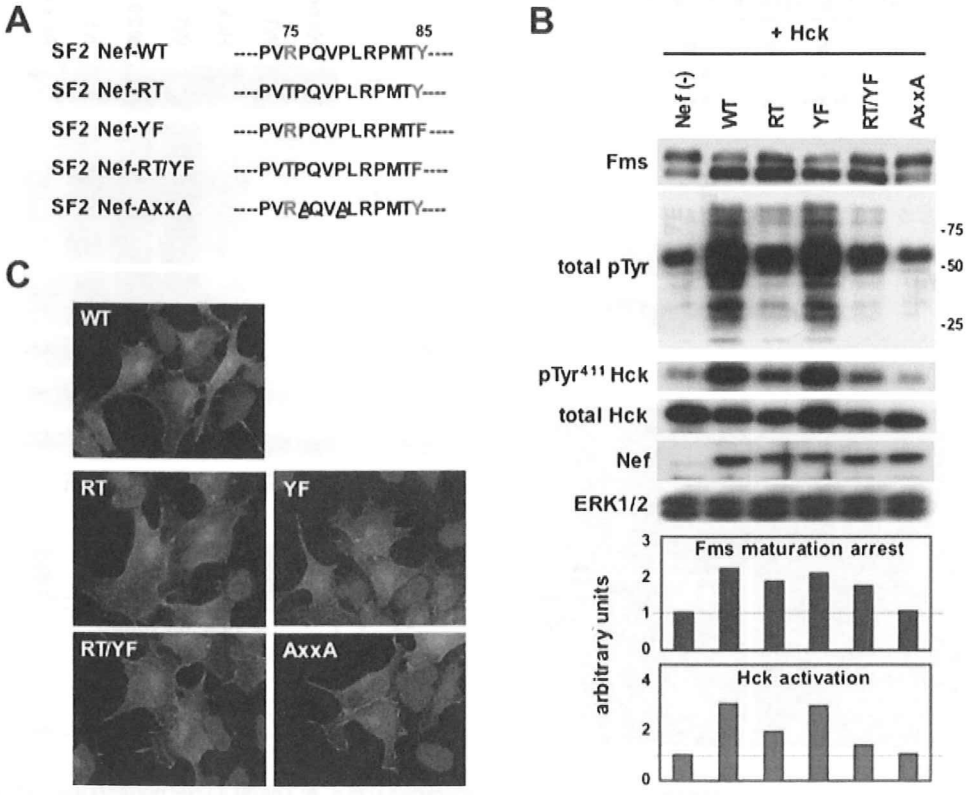

Fig. 4. Abilities of SF2 Nef mutants to activate Hck and to induce Fms maturation arrest. A: The SF2 Nef mutants used (RT, YF, RT/YF, and AxxA) are schematically shown. B: HEK293 cells were transfected with Fms plasmid alone (None) or in combination with the plasmids for Nef and Hck, as indicated. These cells were then analyzed for the expression of Fms, phosphotyrosine (total pTyr), active-Hck ($pTyr^{411}$ Hck), total Hck, GFP-Nef (Nef), or ERK by Western blotting. The quantified Fms maturation arrest and Hck activation are shown in the bar graphs. C: Cells were transfected with indicated GFP-Nef plasmid (green). Nuclei were stained with DAPI (blue). [Color figure can be viewed in the online issue, which is available at www.interscience.wiley.com.]

the Golgi with higher affinity and thereby induced stronger Hck activation and more severe Fms maturation arrest.

There was a single amino acid difference within the PxxP motif, Thr^{71} in NL43 Nef and Arg^{75} in SF2 Nef (Fig. 3A). We found that an NL43 Nef with $Thr^{71}Arg$ substitution (NL43 Nef-TR) showed higher affinity to Hck than wild-type NL43 Nef (Fig. 3B), and induced stronger Hck activation (Fig. 3C) and more severe Fms maturation arrest (Fig. 3D) than wild-type NL43 Nef. We also performed a complementary experiment with SF2 Nef mutants (Fig. 4A; Ueno et al., 2008). As a result, we found that mutants with $Arg^{75}Thr$ substitution (SF2 Nef-RT and SF2-RT/YF) induced moderate Hck activation/Fms maturation arrest (Fig. 4B). However, both showed no obvious change in the pattern of predominant Golgi-localization (Fig. 4C). These results indicated that the single amino acid difference (Thr to Arg) within the PxxP motif governed the higher ability of SF2 Nef to induce Golgi-localization and activation of Hck, and Fms maturation arrest.

Although PxxP motif is essential for Nef to bind Hck, a recent study showed that an acidic region of Nef facilitated Nef-Hck binding at the Golgi (Hung et al., 2007). Although an NL43 Nef mutant lacking this region (ΔE; Fig. 5A) bound GST-Hck SH3 fusion proteins as with wild-type NL43 Nef (Fig. 5B), ΔE mutant was indeed less active than wild-type in transfected HEK293 cells, that is, in both Hck and activation Fms maturation arrest (Fig. 5C). Another mutant (M20; Fig. 5A), which was defective in the down-regulation of MHC I, another hallmark function of Nef (Akari et al., 2000), retained the ability to induce Hck activation and Fms maturation arrest (Fig. 5C). Both ΔE and M20A mutants showed no obvious change in the pattern of predominant Golgi-localization (Fig. 5C). The result further supported the idea that stronger Hck activation, which took place at the Golgi, induced severe Fms maturation arrest.

Analyses with a newly discovered Nef-Hck binding blocker

To directly show that the Golgi-localization of active Hck determines Nef-induced Fms maturation arrest, we sought to discover Nef-Hck binding blockers. In this study, we focused on UCS15A and its analogs 2b and 2c (Fig. 6A), because these small-molecule compounds were shown to block several proline-rich motif-SH3 domain binding such as Sam68-Fyn binding (Oneyama et al., 2003) and AMAP1-cortactin binding (Hashimoto et al., 2006). As they have not been used before for HIV-1 studies, we tested their capability to block Nef-Hck binding by the GST pull-down assay. As shown (Fig. 6B), all compounds blocked the binding of Hck to NL43 Nef or NL43 Nef-TR mutant (more potent than the wild-type, see Fig. 3), in a dose-dependent manner. Like the case of Sam68-Fyn binding (Oneyama et al., 2003), 2c was the most effective in blocking Nef-Hck binding (Fig. 6B), and showed no obvious toxicity to HEK293 cells (Fig. 6C). As shown (Fig. 6D), 2c indeed inhibited

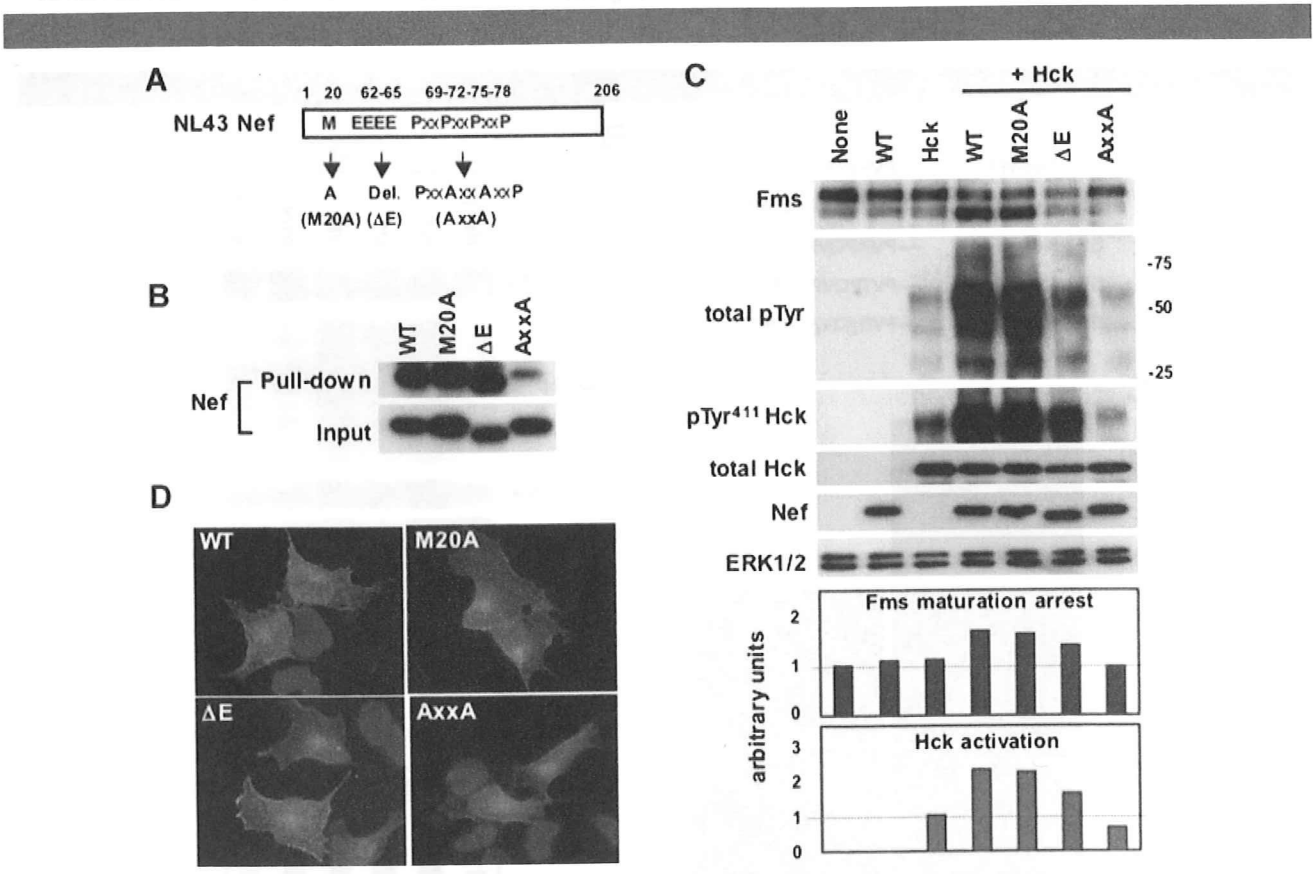

Fig. 5. Abilities of NL43 Nef mutants to activate Hck and to induce Fms maturation arrest. A: The NL43 Nef mutants used (M20A, ΔE, and AxxA) are schematically shown. B: The resin, to which GST-Hck SH3 fusion proteins were bound, were incubated with the lysates of HEK293 cells expressing the indicated Nef proteins. The amount of Nef proteins in the lysates (Input) or bound to the resins (Pull-down) was verified by Western blotting. C: HEK293 cells were transfected with Fms plasmid alone (None) or in combination with the plasmids for Nef and Hck, as indicated. These cells were then analyzed for the expression of Fms, phosphotyrosine (total pTyr), active-Hck ($pTyr^{411}$ Hck), total Hck, CD8-Nef (Nef), or ERK by Western blotting. The quantified Fms maturation arrest and Hck activation are shown in the bar graphs. D: Cells were transfected with indicated GFP-Nef (green). Nuclei were stained with DAPI (blue). [Color figure can be viewed in the online issue, which is available at www.interscience.wiley.com.]

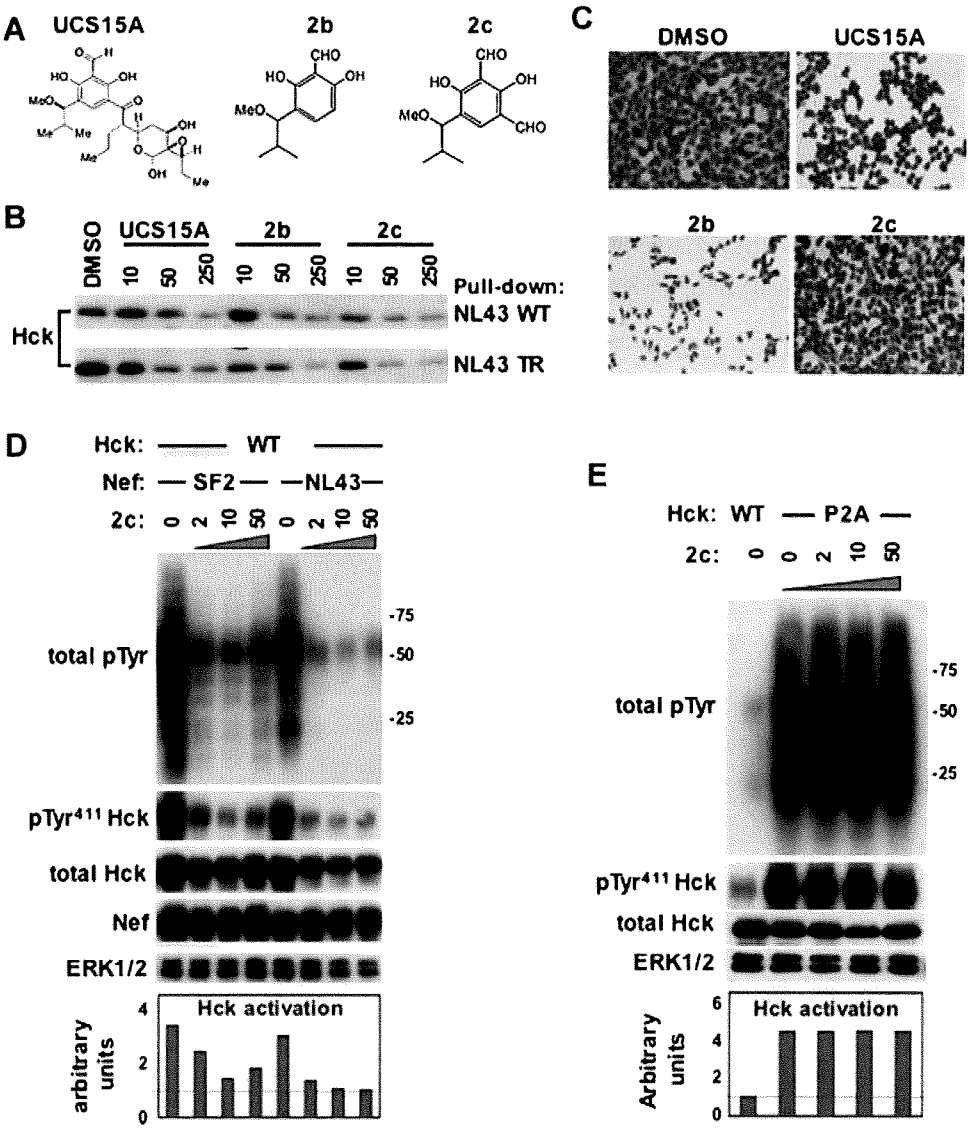

Fig. 6. Capability of 2c to block Nef-Hck binding and Nef-induced Hck activation. A: Chemical structures of UCS15A, 2b, and 2c are shown. B: The resins, to which GST-Nef (NL43 wild-type or TR mutant, see Fig. 2A) proteins were bound, were incubated with the lysates of Hck-expressing HEK293 cells in the absence (DMSO) or presence of the indicated concentration (0, 10, 50, or 250 μM) of UCS15A, 2b, or 2c. The amount of Hck proteins bound to the resins was determined by Western blotting. C: HEK293 cells were cultured in the absence (DMSO) or presence of 50 μM of UCS15A, 2b, or 2c for 2 days, and subjected to Wright-Giemsa staining. D: Cells were co-transfected with Hck-WT and indicated Nef alleles (SF2 or NL43), and cultured in the presence of increasing concentrations (μM) of 2c. These cells were then analyzed for the expression of tyrosine-phosphorylated proteins (total pTyr), active-Hck (pTyr^{411}Hck), total Hck, CD8-Nef (Nef), or ERK by Western blotting. The quantified Hck activation is shown in the bar graphs. E: Cells were transfected with Hck-WT or Hck-P2A, and cultured in the presence of increasing concentrations (μM) of 2c. These cells were analyzed as in (D). [Color figure can be viewed in the online issue, which is available at www.interscience.wiley.com.]

Hck activation by NL43 Nef and more potent SF2 Nef (see Fig. 3). Importantly, 2c had little inhibitory effect on kinase activity of the constitutive-active Hck P2A mutant, even when used at a concentration as high as 50 μM (Fig. 6E). These results indicated that 2c was not a kinase inhibitor but inhibited Nef-induced Hck activation by blocking Nef-Hck binding.

This unique feature of 2c prompted us to examine whether 2c blocks Nef/Hck-induced Fms maturation arrest and Nef-induced skewed Golgi-localization of Hck. As shown (Fig. 7A), 2c completely blocked Fms maturation arrest induced by Nef and wild-type Hck as expected. However, of particular importance was that 2c also completely blocked severe Fms maturation arrest induced by Nef and the constitutive-active Hck P2A (Fig. 7B). Because 2c had little inhibitory effect on kinase activity of Hck-P2A (see Fig. 6E), these results strongly supported that the presence of Hck-P2A at the Golgi caused by its binding with Nef (see Fig. 2) was a direct cause of severe Fms maturation arrest. We therefore sought to verify that 2c indeed blocked Nef-induced skewed Golgi-localization of Hck-P2A. To this end, we employed the quantitative analysis, that is, subcellular fractionation on sucrose gradients (see Fig. 2B). The peak of Hck-P2A shifted to heavier fractions by the co-expression with Nef, and such change in the intracellular localization of Hck-P2A was restored to normal by the addition of 2c (Fig. 7C). We also tested whether 2c blocked Nef-induced Fms abnormality in another culture system. We previously showed that the cell surface expression of Fms was impaired in human myeloid TF-1-fms cells expressing a conditionally active

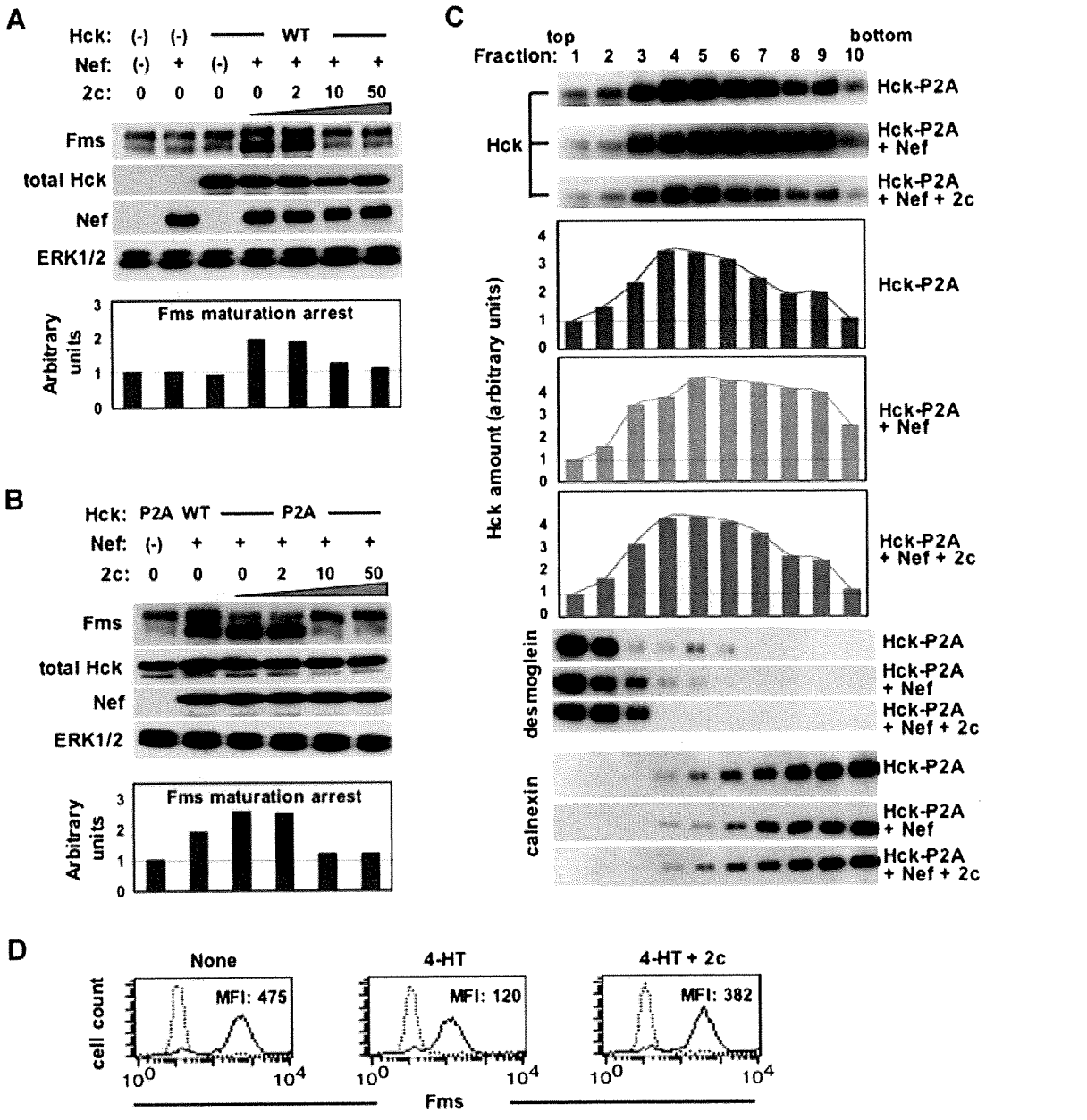

Fig. 7. Capability of 2c to block Fms maturation arrest and skewed Golgi-localization of Hck. A: HEK293 cells were transfected with the plasmids (Fms, NL43 Nef, and Hck-WT) in combination indicated, and cultured in the presence of increasing concentrations (μM) of 2c. These cells were then analyzed for the expression of Fms, total Hck, CD8-Nef (Nef), or ERK by Western blotting. The quantified Fms maturation arrest is shown in the bar graphs. B: Cells were transfected with the plasmids (Fms, NL43 Nef, Hck-WT, and Hck-P2A) in combination indicated, and cultured in the presence of increasing concentrations (μM) of 2c. These cells were then analyzed as in A. C: Cells were transfected with Hck-P2A alone (top), or co-transfected with NL43 Nef (middle). 2c was added to a final concentration of 50 μM to selected wells (bottom). Then, cells were subjected to subcellular fractionation on sucrose gradients and Hck Western blotting. The quantified Hck amounts are shown in the bar graph. The fractions were also analyzed for the amount of desmoglein and calnexin. D: TF-1-fms-Nef-ER cells cultured with M-CSF-free media in the absence (left) or presence of 0.1 μM 4-HT (middle), or the co-presence of 0.1 μM 4-HT and 50 μM 2c (right) for 12 h. The expression of Fms on the surface of treated cells was analyzed by flow cytometry with PE-labeled anti-Fms. The mean fluorescence intensity (MFI) of Fms expression is indicated. [Color figure can be viewed in the online issue, which is available at www.interscience.wiley.com.]

Nef-ER fusion protein when the Nef-ER in the cells was activated by the estrogen analog 4-HT (Hiyoshi et al., 2008). This impaired cell surface Fms expression was highly likely due to intracellular Fms maturation arrest (Hiyoshi et al., 2008). Finally, we found that the Fms down-regulation in Nef-active TF-1-fms-Nef-ER cells was also restored to normal by the addition of 2c (Fig. 7D). All taken together, our present study clearly demonstrated that skewed Golgi-localization of active Hck induced by Nef was indeed the direct cause of Fms maturation arrest.

Discussion

M-CSF is a cytokine essential not only for the survival of macrophages but also for the maintenance of macrophages at an

anti-inflammatory state (reviewed in Chitu and Stanley, 2006; Hamilton, 2008). Thus, the inhibitory effect of Nef on M-CSF signal through Fms maturation arrest at the Golgi is a possible trigger to worsen uncontrolled immune systems in patients (Suzu et al., 2005; Hiyoshi et al., 2008). In this study, we therefore sought to define molecular basis of this important function of Nef, by using different Nef alleles, various Nef mutants, constitutive-active Hck mutant, and Nef-Hck binding blocker 2c. The study with various Nef proteins supported the idea that high affinity Nef-Hck binding and subsequent stronger Hck activation, both of which took place mainly at the Golgi, determined Fms maturation arrest at the Golgi (Figs. 2–5). Moreover, the study with 2c enabled us to conclude that skewed Golgi-localization of active Hck by Nef was indeed the direct cause of Fms maturation arrest (Figs. 6 and 7). By analogy with the Sam68-Fyn binding inhibition (Oneyama et al., 2003), the inhibitory effect of 2c on Nef-Hck binding was supposed to be mediated by its interaction with Nef PxxP motif.

As mentioned earlier, it has been known for a long time that most members of Src kinases including Hck localize to the Golgi as well as to the plasma membrane. For example, it was shown that newly synthesized Lyn initially localized and accumulated to the Golgi, and then moved toward the plasma membrane (Kasahara et al., 2004). Importantly, Pulvirenti et al. (2008) recently revealed that coordinated regulation of activity of the Golgi-localized Src kinases is crucial to maintain intra-Golgi trafficking of proteins. Our present finding that skewed Golgi-localization of active Hck leads to Fms maturation arrest at the Golgi is in line with the new concept. It appears that long-lasting and dys-regulated activation of the Golgi-localized Src kinases disturbs glycosylation and/or trafficking of proteins, exemplified by Fms maturation arrest. Indeed, N-Src, a c-Src isoform with a higher basal tyrosine kinase activity (Brugge et al., 1985), showed more obvious perinuclear localization than the constitutive-active Hck-P2A and induced Fms maturation arrest even in the absence of Nef (unpublished result). Moreover, Mitina et al. (2007) reported that over-expression of an active form of Hck disturbed *N*-glycosylation of another cytokine receptor Flt3 even in the absence of Nef. These results may further support the idea that long-lasting and dys-regulated activation of the Golgi-localized Src kinases per se affects protein glycosylation and/or trafficking at the Golgi. Anyhow, our system with Nef provides a useful model to elucidate how Src kinases regulate the Golgi structure/function. It will be important to identify which Golgi proteins are phosphorylated directly or indirectly by Hck activated at the Golgi and to clarify how such phosphorylation cascade leads to Nef-induced Fms maturation arrest.

Nef has been shown to affect protein trafficking and a well-characterized target is major histocompatibility complex class I (MHC I). Nef reduced the cell surface expression of MHC I, which diminishes the recognition of infected cells by cytotoxic T cells (reviewed in Fackler and Baur, 2002; Peterlin and Trono, 2003). However, it is still in intense debate whether Nef requires SH3 domain-containing proteins such as Hck to reduce the cell surface level of MHC I (Schwartz et al., 1996; Greenberg et al., 1998; Mangasarian et al., 1999; Akari et al., 2000; Chang et al., 2001; Roeth and Collins, 2006; Hung et al., 2007; Atkins et al., 2008). In this regard, Fms is not the direct target of Nef. However, as shown, Nef disturbed the cell surface expression of Fms, which is triggered by skewed Golgi-localization of active Hck. Moreover, it was shown that Nef disturbed the cell surface expression of another macrophage-specific protein HFE, an iron homeostasis regulator, which was blocked by a dominant-negative Hck (Drakesmith et al., 2005). Although whether the reduced cell surface level of HFE by Nef relates to skewed Golgi-localization of active Hck is unclear, it is conceivable that Nef acquires an additional machinery to manipulate protein trafficking in macrophages by exploiting the Golgi-localized Hck. Of interest, the *N*-glycosylation of Flt3, which is structurally related to Fms, was also impaired in Nef/Hck-expressing HEK293 cells, but the degree of maturation arrest of Flt3 was quite weak when compared to that of Fms (data not shown). The finding may imply that Fms maturation arrest is not necessarily due to the general disruption in the Golgi structure or function. Future studies, in which we determine to what extent overall protein *N*-glycosylation and trafficking are affected by Nef-Hck binding, will further clarify pathological significance of the molecular binding in macrophages. The newly discovered Nef-Hck binding blocker 2c will be useful in such studies and may provide a strategy to complement current anti-HIV-1 therapy for better treatment outcomes.

In this study, we showed that SF2 Nef had much higher affinity to Hck than NL43 Nef and thereby induced stronger Hck activation/severe Golgi-localization of Hck (Figs. 2 and 3) and that the single amino acid difference (Thr^{71} in NL43 Nef and Arg^{75} in SF2 Nef) within PxxP motif largely governs the higher ability of SF2 Nef (Figs. 3 and 4). This difference might reflect that the $Thr^{71}Arg$ substitution in NL43 Nef (NL43 Nef-TR, see Fig. 3) altered the flexibility of a loop containing the PxxP motif (Fackler et al., 2001). Importantly, for reasons not clearly understood, NL43 Nef-TR was more pathogenic in HIV-1 Tg mice than wild-type NL43 Nef and the pathogenicity of SF2 Nef in Tg mice was evident despite very low levels of expression (Priceputu et al., 2007). It is therefore possible that more severe Golgi-localization of active Hck followed by perturbed *N*-glycosylation and trafficking of proteins including Fms account for the high pathogenicity of SF2 Nef in Tg mice.

In summary, our present study clearly demonstrated that skewed Golgi-localization of active Hck was the direct cause of Fms maturation arrest by Nef. Our findings establishes an intriguing link between the pathogenesis of HIV-1 Nef and the newly emerging concept that the Golgi-localized Src kinases regulate the Golgi function. The identification of Golgi proteins phosphorylated by the Golgi-localized active Hck will provide novel insights into molecular mechanisms by which Nef functions as an HIV-1 pathogenetic factor through Hck and the Gogi-localized Src kinases regulate the Golgi function.

Acknowledgments

We thank Dr. G. Thomas (Vollum Institute) for critical reading of the manuscript. We thank Ms. Y. Endo and Ms. I. Suzu for experimental assistance.

Literature Cited

Akari H, Arold S, Fukumori T, Okazaki T, Strebel K, Adachi A. 2000. Nef-induced major histocompatibility complex class I down-regulation is functionally dissociated from its virion incorporation, enhancement of viral infectivity, and CD4 down-regulation. J Virol 74:2907–2912.

Arold S, O'Brien R, Franken P, Strub MP, Hoh F, Dumas C, Ladbury JE. 1998. RT loop flexibility enhances the specificity of Src family SH3 domains for HIV-1 Nef. Biochemistry 37:14683–14691.

Atkins KM, Thomas L, Youker RT, Harriff MJ, Pissani F, You H, Thomas G. 2008. HIV-1 Nef binds PACS-2 to assemble a multikinase cascade that triggers major histocompatibility complex class I (MHC-I) down-regulation: Analysis using short interfering RNA and knock-out mice. J Biol Chem 283:11772–11784.

Bard F, Mazelin L, Pechoux-Longin C, Malhotra V, Jurdic P. 2003. Src regulates Golgi structure and KDEL receptor-dependent retrograde transport to the endoplasmic reticulum. J Biol Chem 278:46601–46606.

Bijlmakers MJ, Isobe-Nakamura M, Ruddock LJ, Marsh M. 1997. Intrinsic signals in the unique domain target p56lck to the plasma membrane independently of CD4. J Cell Biol 137:1029–1040.

Brugge JS, Cotton PC, Queral AE, Barrett JN, Nonner D, Keane RW. 1985. Neurones express high lenels of a structurally modified, activated form of pp60c-src. Nature 316:554–557.

Carreno S, Gouze ME, Schaak S, Emorine LJ, Maridonneau-Parini I. 2000. Lack of palmitoylation redirects $p59^{Hck}$ from the plasma membrane to $p61^{Hck}$-positive lysosomes. J Biol Chem 275:36223–36229.

Chang AH, O'Shaughnessy MV, Jirik FR. 2001. Hck SH3 domain-dependent abrogation of Nef-induced class I MHC down-regulation. Eur J Immunol 31:2382–2387.

Chitu V, Stanley ER. 2006. Colony-stimulating factor-1 in immunity and inflammation. Curr Opin Immunol 18:39–48.

David-Pfeuty T, Nouvian-Dooghe Y. 1990. Immunolocalization of the cellular src protein in interphase and mitotic NIH c-src overexpresser cells. J Cell Biol 111:3097–3116.
Deacon NJ, Tsykin A, Solomon A, Smith K, Ludford-Menting M, Hooker DJ, McPhee DA, Greenway AL, Ellett A, Chatfield C, Lawson VA, Crowe S, Maerz A, Sonza S, Learmont, Sullivan JS, Cunningham A, Dwyer D, Mills J. 1995. Genomic structure of an attenuated quasi species of HIV-1 from a blood transfusion and recipients. Science 270:988–991.
Drakesmith H, Chen N, Ledermann H, Screaton G, Townsend A, Xu XN. 2005. HIV-1 Nef down-regulates the hemochromatosis protein HFE, manipulating cellular iron homeostasis. Proc Natl Acad Sci USA 102:11017–11022.
Fackler OT, Baur AS. 2002. Live and let die: Nef functions beyond HIV replication. Immunity 16:493–497.
Fackler OT, Wolf D, Weber HO, Laffert B, D'Aloja P, Schuler-Thurner B, Geffin R, Saksela K, Geyer M, Peterlin BM, Schuler G, Baur AS. 2001. A natural variability in the proline-rich motif of Nef modulates HIV-1 replication in primary T cells. Curr Biol 11:1294–1299.
Greenberg ME, Iafrate AJ, Skowronski J. 1998. The SH3 domain-binding surface and an acidic motif in HIV-1 nef regulate trafficking of class I MHC complexes. EMBO J 17:2777–2789.
Haller C, Rauch S, Fackler OT. 2007. HIV-1 Nef employs two distinct mechanisms to modulate Lck subcellular localization and TCR induced actin remodeling. PLoS ONE 2:e1212.
Hamilton JA. 2008. Colony-stimulating factors in inflammation and autoimmunity. Nat Rev Immunol 8:533–544.
Hanna Z, Kay DG, Rebai N, Guimond A, Jothy S, Jolicoeur P. 1998. Nef harbors a major determinant of pathogenicity for and AIDS-like disease induced by HIV-1 in transgenic mice. Cell 95:163–175.
Hanna Z, Weng X, Kay DG, Poudrier J, Lowell C, Jolicoeur P. 2001. The pathogenicity of human immunodeficiency virus (HIV) type 1 Nef in CD4C/HIV transgenic mice is fabolished by mutation of its SH3-binding domain, and disease development is delayed in the absence of Hck. J Virol 75:9378–9392.
Hashimoto S, Hirose M, Hashimoto A, Morishige M, Yamada A, Hosaka H, Akagi K, Ogawa E, Oneyama C, Agatsuma T, Okada M, Kobayashi H, Wada H, Nakano H, Ikegami T, Nakagawa A, Sabe H. 2006. Targeting AMAP1 and cortactin binding bearing an atypical src homology 3/proline interface for prevention of breast cancer invasion and metastasis. Proc Natl Acad Sci USA 103:7036–7041.
Hiyoshi M, Suzu S, Yoshidomi Y, Hassan R, Harada H, Sakashita N, Akari H, Motoyoshi K, Okada S. 2008. Interaction between Hck and HIV-1 Nef negatively regulates cell surface expression of M-CSF receptor. Blood 111:243–250.
Hung CH, Thomas L, Ruby CE, Atkins KM, Morris NP, Knight ZA, Scholz I, Barklis E, Weinberg AD, Shokat KM, Thomas G. 2007. HIV-1 Nef assembles a Src family kinase-ZAP-70/Syk-PI3K cascade to down-regulate cell surface MHC-I. Cell Host Microbe 1:121–133.
Kaplan KB, Swedlow JR, Varmus HE, Morgan DO. 1992. Association of $p60^{c\text{-}src}$ with endosomal membranes in mammalian fibroblasts. J Cell Biol 118:321–333.
Karkkainen S, Hiipakka M, Wang JH, Kleino I, Vaha-Jaakkola M, Renkema GH, Kiss M, Wagner R, Saksela K. 2006. Identification of preferred protein interactions by phage-display of the human Src homology-3 proteome. EMBO Rep 7:186–191.
Kasahara K, Nakayama Y, Ikeda K, Fukushima Y, Matsuda D, Horimoto S, Yamaguchi N. 2004. Trafficking of Lyn through the Golgi caveolin involves the charged residues on αE and αI helices in the kinase domain. J Cell Biol 165:641–652.
Kestler HW III, Ringler DJ, Mori K, Panicali DL, Sehgal PK, Daniel MD, Desrosiers RC. 1991. Importance of the nef gene for maintenance of high virus loads and for development of AIDS. Cell 65:651–662.
Kirchhoff F, Greenough TC, Brettler DB, Sullivan JL, Desrosiers RC. 1995. Brief report: Absence of intact nef sequences in a long-term survivor with nonprogressive HIV-1 infection. N Engl J Med 332:228–232.
Korade-Mirnics Z, Corey SJ. 2000. Src kinase-mediated signaling in leukocytes. J Leukocyte Biol 68:603–613.
Lerner EC, Smithgall TE. 2002. SH3-dependent stimulation of Src-family kinase autophosphorylation without tail release from the SH2 domain in vivo. Nat Struct Biol 9:365–369.
Ley SC, Marsh M, Bebbington CR, Proudfoot K, Jordan P. 1994. Distinct intracellular localization of Lck and Fyn protein tyrosine kinases in human T lymphocytes. J Cell Biol 125:639–649.
Lowell CA. 2004. Src-family kinases: Rheostats of immune cell signaling. Mol Immunol 41:631–643.
Mangasarian A, Piguet V, Wang JK, Chen YL, Trono D. 1999. Nef-induced CD4 and major histocompatibility complex class I (MHC-I) down-regulation are governed by distinct determinants: N-terminal alpha helix and proline repeat of Nef selectively regulate MHC-I trafficking. J Virol 73:1964–1973.
Matsuda D, Nakayama Y, Horimoto S, Kuga T, Ikeda K, Kasahara K, Yamaguchi N. 2006. Involvement of Golgi-associated Lyn tyrosine kinase in the translocation of annexin II to the endoplasmic reticulum under oxidative stress. Exp Cell Res 312:1205–1217.
Mitina O, Warmuth M, Krause G, Hallek M, Obermeier A. 2007. Src family tyrosine kinases phosphorylate Flt3 on juxtamembrane tyrosines and interfere with receptor maturation in a kinase-dependent manner. Ann Hematol 86:777–785.
Moarefi I, LaFevre-Bernt M, Sicheri F, Huse M, Lee CH, Kuriyan J, Miller WT. 1997. Activation of the Src-family tyrosine kianse Hck by SH3 domain displacement. Nature 385:650–653.
Oneyama C, Agatsuma T, Kanda Y, Nakano H, Sharma SV, Nakano S, Narazaki F, Tatsuta K. 2003. Synthetic inhibitors of proline-rich ligand-mediated protein-protein interaction: Potent analogs of UCS15A. Chem Biol 10:443–451.
Paliwal P, Radha V, Swarup G. 2007. Regulation of p73 by Hck through kinase-dependent and independent mechanisms. BMC Mol Biol 8:45.
Peterlin BM, Trono D. 2003. Hide, shield and strike back: How HIV-infected cells avoid immune eradication. Nat Rev Immunol 3:97–107.
Priceputu E, Hanna Z, Hu C, Simard MC, Vincent P, Wildum S, Schindler M, Kirchhoff F, Jolicoeur P. 2007. Primary human immunodeficiency virus type 1 Nef alleles show major differences in pathogenicity in transgenic mice. J Virol 81:4677–4693.
Pulvirenti T, Giannotta M, Capestrano M, Capitani M, Pisanu A, Polishchuk RS, San Pietro E, Beznoussenko GV, Mironov AA, Turacchio G, Hsu VW, Sallese M, Luini A. 2008. A traffic-activated Golgi-based signaling circuit coordinates the secretory pathway. Nat Cell Biol 10:912–922.
Roeth JF, Collins KL. 2006. Human immunodeficiency virus type 1 Nef: Adapting to intracellular trafficking pathways. Mol Biol Rev 70:548–563.
Saksela K, Cheng G, Baltimore D. 1995. Proline-rich (PxxP) motifs in HIV-1 Nef bind to SH3 domains of a subset of Src kinases and are required for the enhanced growth of Nef^{+} viruses but not for down-regulation of CD4. EMBO J 14:484–491.
Schwartz O, Marechal V, Le Gall S, Lemonnier F, Heard JM. 1996. Endocytosis of major histocompatibility complex class I molecules is induced by the HIV-1 Nef protein. Nat Med 2:338–342.
Suzu S, Tanaka-Douzono M, Nomaguchi K, Yamada M, Hayasawa K, Kimura F, Motoyoshi K. 2000. $p56^{dok\text{-}2}$ as a cytokine-inducible inhibitor of cell proliferation and signal transduction. EMBO J 19:5114–5122.
Suzu S, Harada H, Matsumoto T, Okada S. 2005. HIV-1 Nef interferes with M-CSF receptor signaling through Hck activation and inhibits M-CSF bioactivities. Blood 105:3230–3237.
Trible RP, Emert-Sedlak L, Smithgall TE. 2006. HIV-1 Nef selecyively activates Src family kinases Hck, Lyn, and c-Src through SH3 domain interaction. J Biol Chem 281:27029–27038.
Ueno T, Motozono C, Dohki S, Mwimanzi P, Rauch S, Fackler OT, Oka S, Takiguchi M. 2008. CTL-mediated selective pressure influences dynamic evolution and pathogenetic functions of HIV-1 Nef. J Immunol 180:1107–1116.
van't Hof W, Resh MD. 1997. Rapid plasma membrane anchoring of newly synthesized p59fyn: Selective requirement for NH_2-terminal myristoylation and palmitoylation at cysteine-3. J Cell Biol 136:1023–1035.